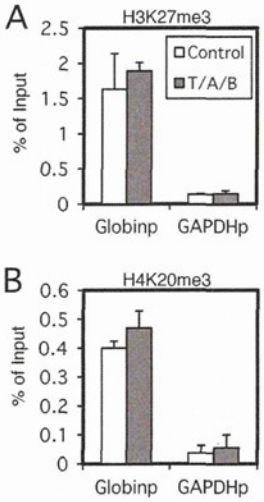

FIG 2 Effect of lytic induction on cellular promoters. Raji cells were treated with TPA (20 ng/ml), A23187 (1 μM), and sodium butyrate (5 mM) (T/A/B; gray bar) or with the vehicle (Control; white bar) for 20 h. Cells then were cross-linked, and ChIP experiments were performed using anti-histone H3K27me3 (A) or anti-H4K20me3 (B) antibody, followed by DNA extraction and real-time PCR to detect DNA fragments using the primers as indicated.

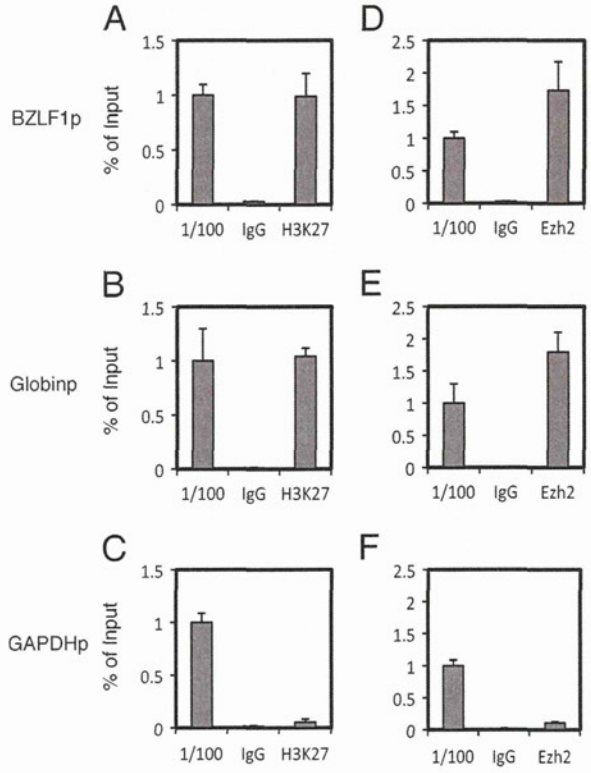

FIG 3 Presence of H3K27me3 and Ezh2 in Raji cells. ChIP experiments were carried out using lysates from Raji cells latently infected with EBV. Cross-linked DNA-protein complexes were precipitated using normal IgG, anti-H3K27me3 antibody (A to C), or anti-Ezh2 antibody (D to F), followed by DNA extraction and real-time PCR analysis for quantification using the indicated primers.

H3K27me3 (Fig. 2A) and H4K20me3 (Fig. 2B) modifications at the β-globin promoter (Globinp) and GAPDH promoter (GAPDHp) in Raji cells. The levels of histone modifications at the cellular promoters, however, did not appreciably change by lytic induction, thus the normalization of the ChIP data to an internal control do not make a significant change in the result that levels of the repressive marks did not diminish (Fig. 1E to H). Recently, Ramasubramanyan and others proved the presence of histone H3K9me3 and H3K27me3 at the Zp and oryLyt in the latent EBV genome of Akata cells (47), where they clearly demonstrated that lytic induction caused an increase of phosphorylated histone H2AX; however, they did not show the decrease of H3K9me3 and H3K27me3.

Presence of the repressive H3K27me3 marker and Ezh2 in the BZLF1 promoter. Since epigenetic analyses of other herpesviruses, including HSV (7, 32) and KSHV (18, 52), have implicated the repressive histone H3K27me3 marker in the maintenance of viral latency, we sought to further examine this modification in the BZLF1 promoter of EBV by ChIP assays (Fig. 3). For detection, we used a set of specific primers that amplify minimal the BZLF1 promoter (−221 to +12; identical to Zp0 in Fig. 1), which is required for the transcriptional activation of the gene in response to TPA or anti-Ig. The histone H3K27me3 modification level of the Zp (0.99% of input) (Fig. 3A) was almost comparable to that of the β-globin promoter (1.0) (Fig. 3B) when the modification of the GAPDH promoter was markedly low (0.053%) (Fig. 3C) in Raji cells. Since it is known that the β-globin locus is marked by a high level of H3K27me3 in nonerythroid cells and the locus of GAPDH, a typical housekeeping gene, is highly demethylated at H3K27 (26), we conclude that the Zp is modified by H3K27me3.

To further test this conclusion, we tested if Ezh2, the enzyme responsible for H3K27 trimethylation (5), associates with Zp. Ezh2 was detected at a very low level at the GAPDHp (0.11% of input) (Fig. 3F), but the detection levels were substantially higher at the Zp (1.7%) (Fig. 3D) and Globinp (1.8%) (Fig. 3E). Therefore, the association of Ezh2 was correlated with the levels of the H3K27me3 marker in Raji cells.

Panels of cell lines latently infected with EBV were tested for H3K27me3: B cells (Akata and LCL EBV-BAC), NK cells (SNK6), and epithelial cells (293EBV-BAC). Depending on the cell type, 0.35 to 1.64% of the promoter region in the input lysate was coprecipitated with H3K27me3 antibody, while normal IgG failed to pull down the promoter sequence (Fig. 4). Histone H3K27me3 levels at the Zp were comparable to those at the β-globin promoter and were notably higher than those at the GAPDH promoter (Fig. 4). Therefore, histone H3K27me3 modification is present in the Zp of EBV, as in other herpesviruses.

Presence of the repressive H4K20me3 marker in the BZLF1 promoter. We then proved that another repressive marker, histone H4K20me3, is present at the Zp by comparing to control promoters in Raji cells (Fig. 5). The presence of the mark at the Zp (1.1% of input) (Fig. 5A) as well as at the Globinp (0.81%) (Fig. 5B) was confirmed, whereas the GAPDH promoter was not efficiently coprecipitated with H4K20me3 antibody (0.065%) (Fig. 5C).

We then checked if the H4K20me3 modification was present in other EBV-positive cell lines (Fig. 6). To our knowledge, the presence of the H4K20me3 marker of promoters of key molecules that regulate reactivation from latency of any herpesviruses, including EBV, has never been clearly confirmed. ChIP analysis demonstrated that the H4K20me3 methylation in the Zp of EBV in Akata, LCL EBV-BAC, SNK6, and 293EBV-BAC cells was present and

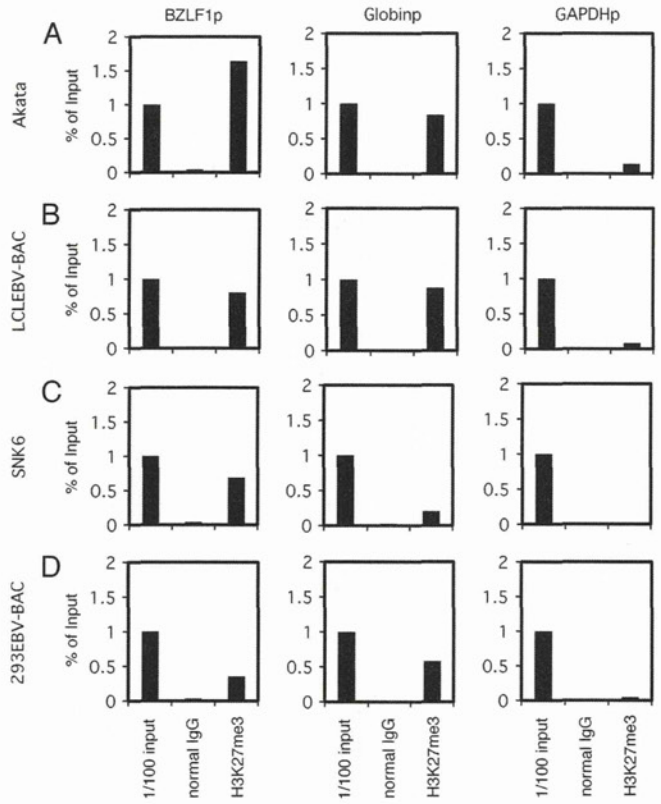

FIG 4 H3K27me3 status in EBV-positive cells. ChIP experiments were carried out using lysates from latent Akata (A), LCLEBV-BAC (B), SNK6 (C), and 293EBV-BAC (D) cells. Cross-linked DNA-protein complexes were precipitated using normal IgG or anti-H3K27me3 antibody, followed by DNA extraction and real-time PCR analysis for quantification using the indicated primers.

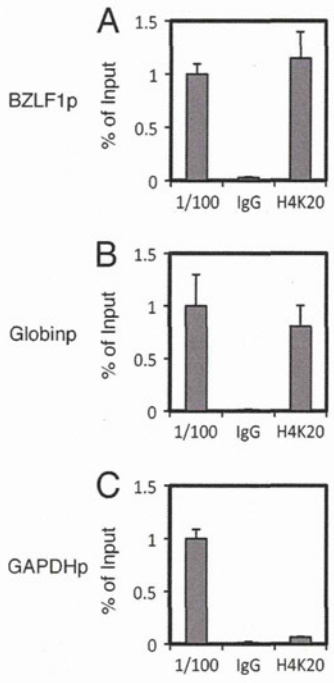

FIG 5 Presence of H4K20me3 in Raji cells. (A to C) ChIP experiments were carried out using lysates from Raji cells latently infected with EBV. Cross-linked DNA-protein complexes were precipitated using normal IgG or anti-H4K20me3 antibody, followed by DNA extraction and real-time PCR analysis for quantification using the indicated primers.

was comparable to that of the β-globin promoter, whereas the GAPDH promoter was hardly modified by the marker (Fig. 6).

Pharmacological inhibition of H3K27me3 and H4K20me3 by DZNep augments BZLF1 expression with TSA in Raji cells. After confirming the presence of histone H3K27me3 and H4K20me3 in the Zp of EBV, to examine if the repressive mark is actually functional we next used a small molecule, 3-deazaneplanocin A (DZNep), which has been reported to suppress H3K27me3 and H4K20me3 histone modification (39, 51). While the treatment of Raji cells with either DZNep or TSA alone had only minor effects on BZLF1 levels (1.8- and 3.3-fold increase, respectively), the use of the two inhibitors in combination (TSA plus DZNep) stimulated the expression 64.2-fold (Fig. 7A). This result suggests that in Raji cells, not only histone deacetylation but also histone H3K27me3 and H4K20me3 serve to inhibit BZLF1 transcription in collaboration. In addition, we confirmed that 5-Aza, an inhibitor of CpG DNA methylation, clearly upregulates the BZLF1 transcription levels (Fig. 7A) as previously demonstrated (57), yet it is very likely that CpG methylation was not involved in the process (10, 15). As a control, we also examined the levels of EBNA2 mRNA in the same samples (Fig. 7B). EBNA2 is a latent gene abundantly expressed in type III latency, including in Raji cells. As expected, none of the pharmacological inhibitions tested here further markedly induce EBNA2 expression (Fig. 7B), as the levels were intrinsically high. We then confirmed that DZNep treatment effectively and significantly ($P < 0.05$) reduced the levels of H3K27me3 (Fig. 7C) and H4K20me3 (Fig. 7D) in the BZLF1 and β-globin promoters. In addition, we checked H3K27me3, H4K20me3, H3K9Ac, and H3K4me3 markers in the BZLF1 (Fig. 7E), β-globin (Fig. 7F), and GAPDH (Fig. 7G) promoters in Raji cells treated with the inhibitors used for Fig. 7A. DZNep or TSA plus DZNep treatment reduced the H3K27me3 and H4K20me3 levels of the Zp and Globinp (Fig. 7E, F, H3K27me3 and H4K20me3, red and purple bars), while other treatments did not noticeably decrease the modification, confirming the specificity and efficacy of DZNep. The presence of TSA or sodium butyrate (T/A/B) strikingly elevated levels of the active marks H3K9Ac and H3K4me3 at the Zp (Fig. 7E, H3K9Ac and H3K4me3, green, purple, or white). Interestingly, those HDAC inhibitors caused a remarkable increase of H3K9Ac modification at the β-globin promoter, but the H3K4me3 modification of the promoter was not affected (Fig. 7F). We speculate that the behavior of active markers varies a great deal depending on the promoters, and notably the activation of the BZLF1 promoter may be characterized by H3K4me3.

To extend the experiment, we checked BZLF1 expression in other typical EBV-positive cell lines, Akata and B95-8 (Fig. 8). As reported previously (37, 38), the treatment of Akata cells with an HDAC inhibitor, TSA, alone was sufficient to induce BZLF1 transcription (52.6-fold), suggesting that low levels of histone acetylation play an important role in the silencing. On the other hand, TSA alone did not induce BZLF1 transcription in B95-8, suggesting that the molecular mechanisms that govern the suppression of BZLF1 transcription in those cells is more complicated (10, 11, 17). An inhibitor of CpG methylation, 5-Aza, enhanced BZLF1 expression in both cell lines as previously reported (57). Unlike

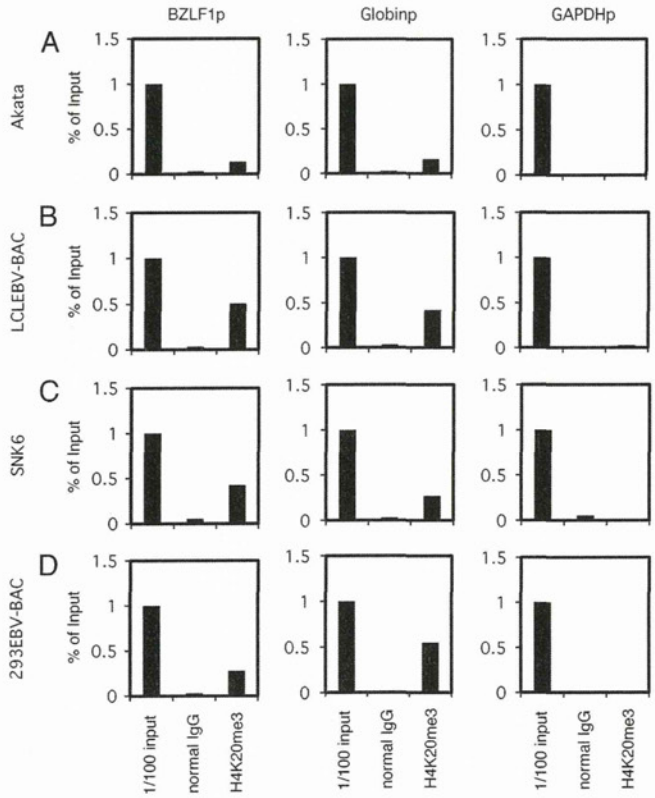

FIG 6 H4K20me3 status of EBV-positive cells. ChIP experiments were carried out using lysates from latent Akata (A), LCLEBV-BAC (B), SNK6 (C), and 293EBV-BAC (D) cells. Cross-linked DNA-protein complexes were precipitated using normal IgG or anti-H4K20me3 antibody, followed by DNA extraction and real-time PCR analysis for quantification using the indicated primers.

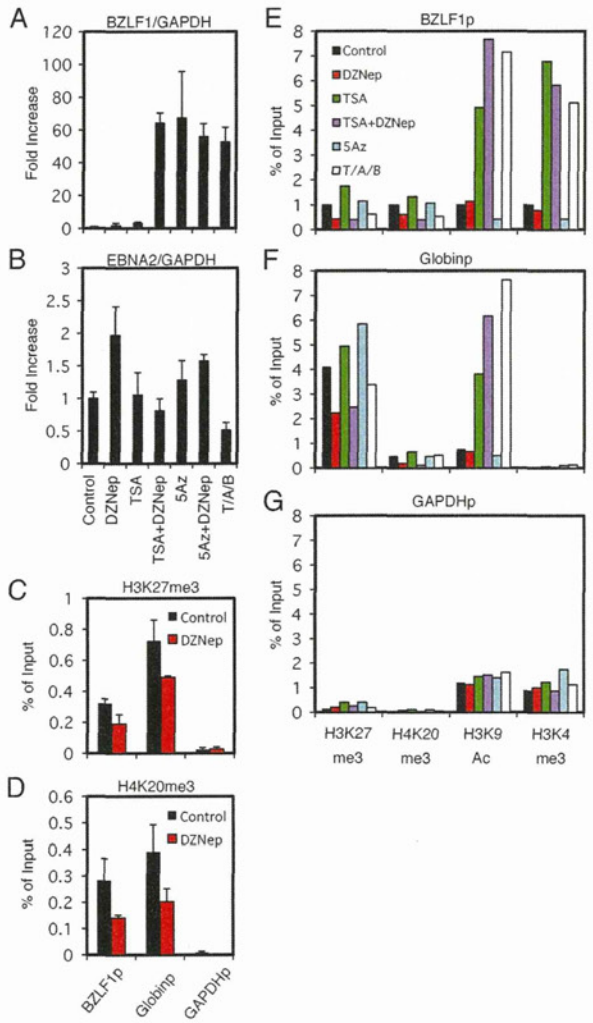

FIG 7 Effects of pharmacological inhibitors on BZLF1 expression. (A and B) Effects of pharmacological inhibitors on BZLF1 expression. Raji cells were treated with either vehicle (Control), 10 μM DZNep (DZ), 300 nM trichostatin A (TSA), 1 μM 5-aza-2′-deoxycytidine (5Az), or in combinations as indicated. As a positive control (T/A/B), Raji cells were treated with 20 ng/ml TPA, 1 μM A23187, and 5 mM sodium butyrate. For DZNep or 5-Aza-2′-deoxycytidine (5Az) treatment, cells were exposed to the reagent daily for 3 days. Treatment with other chemicals was conducted for 24 h. Real-time RT-PCR was carried out as described in Materials and Methods. Levels of BZLF1 (A) and EBNA2 (B) mRNAs were normalized to GAPDH mRNA levels and are shown as fold increase. Each bar represents the means and SD from three independent treatments. (C to G) Effects of pharmacological inhibitors on epigenetic modifications. (C and D) Raji cells treated with DZNep were subjected to ChIP assays using anti-H3K27me3 (C) and anti-H4K20me3 (D) antibodies, followed by DNA extraction and real-time PCR to detect DNA fragments using the indicated primers. (E to G) Raji cells treated with inhibitors in the same way were subjected to ChIP assays using anti-H3K27me3, anti-H4K20me3, anti-H3K9Ac, or anti-H3K4me3 antibody, followed by DNA extraction and real-time PCR to detect DNA fragments using the indicated primers.

Raji cells, both Akata and B95-8 cells did not respond to DZNep, even in combination with TSA or 5-Aza. Notably, EBNA2 is hardly expressed in Akata cells, because the virus takes type I latency and then is induced by 5-Aza as reported previously (15), suggesting that the inhibitor is working as intended.

Knockdown of H3K27me3 methyltransferase Ezh2. We tested small-molecule epigenetic inhibitors in the previous section, and the results strongly suggested the involvement of histone H3K27me3 and H4K20me3 methylations in the maintenance of latency in Raji cells. We next carried out the knockdown of methylation enzymes (Fig. 9 and 10). First, to further confirm the physiological significance of the epigenetic silencing of the BZLF1 gene by histone H3K27me3 in Raji cells, we knocked down Ezh2, the methyltransferase enzyme responsible for the modification (5). As shown in Fig. 9B, the transfection of siRNA against Ezh2 caused a decrease in Ezh2 mRNA levels (54 or 40% of control, without or with TSA, respectively). Accordingly, immunoblotting showed protein levels of Ezh2 to be markedly decreased by the siRNA treatment (Fig. 9C). The silencing of Ezh2 increased BZLF1 levels by 2.5-fold even without TSA, and the addition of TSA elevated this to 10.9-fold (Fig. 9A). The induction of BZLF1 mRNA by si-Ezh2 and TSA was correlated with the reduction of repressive H3K27me3 marker and the increment of active H3K9Ac and H3K4me3 markers (Fig. 9D to H). Taking the results of inhibitor experiments in Fig. 7 into consideration, this result pointed to the involvement of Ezh2 methyltransferase and the histone H3K27me3 mark in the silencing of BZLF1 gene expression during EBV latency. In addition, we note that histone acetylation is also needed for the efficient expression of BZLF1.

Knockdown of H4K20me3 methyltransferase Suv420h1. Results in the previous sections strongly suggested the significance of the repressive H4K20me3 marker for the suppression of Zp. To

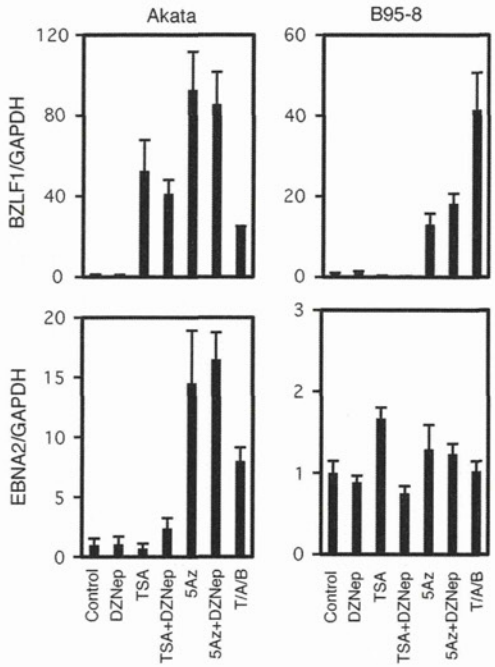

FIG 8 Effects of pharmacological inhibitors on BZLF1 expression in Akata and B95-8 cells. Akata or B95-8 cells were treated with either vehicle (Control), 10 μM DZNep (DZ), 300 nM Trichostatin A (TSA), 1 μM 5-aza-2′-deoxycytidine (5Az), or in combinations as indicated. As positive controls (PC), Akata cells were treated with anti-IgG (10 μg/ml), and B95-8 cells were treated with 20 ng/ml TPA, 1 μM A23187, and 5 mM sodium butyrate. For DZNep or 5Az treatment, cells were exposed to the reagent daily for 3 days. Treatments with other chemicals were conducted for 24 h. Real-time RT-PCR was carried out as described in Materials and Methods. Levels of BZLF1 (upper panels) and EBNA2 (lower panels) mRNAs were normalized to GAPDH mRNA levels and are shown as fold increase. Each bar represents the means and SD from three independent treatments.

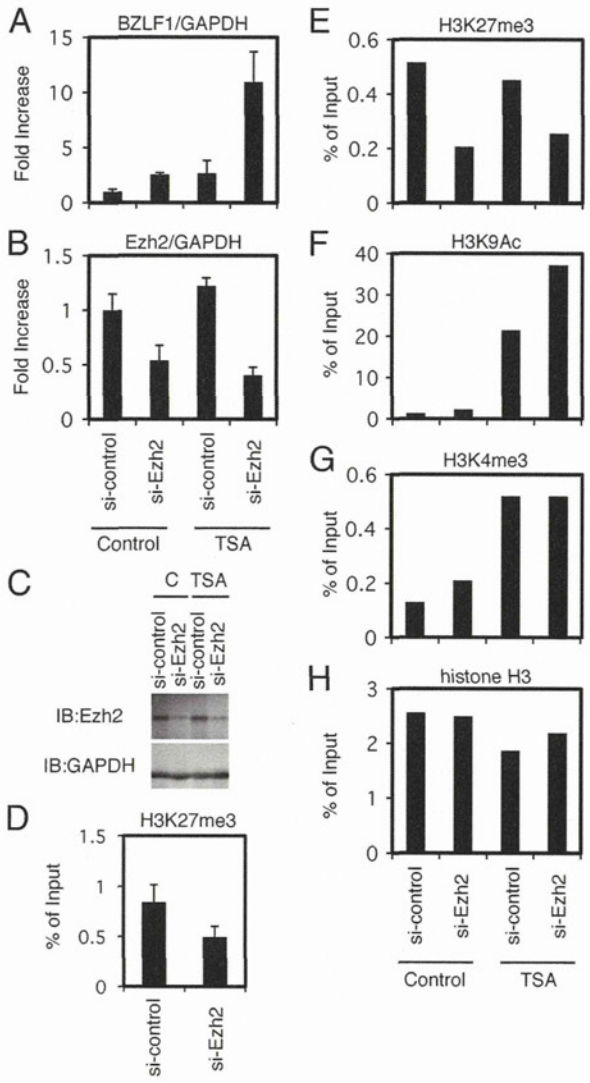

FIG 9 Knockdown of H3K27me3 methyltransferase Ezh2. (A to C) Raji cells transfected with siRNA against Ezh2 (si-Ezh2) or a control siRNA (si-control) were cultured for 48 h and then treated with TSA (300 nM) or vehicle DMSO (Control) for an additional 24 h. Levels of BZLF1 (A) and Ezh2 (B) mRNA were checked by real-time RT-PCR. (C) Levels of Ezh2 protein were examined by immunoblotting. (D to H) Epigenetic status of the Zp after Ezh2 knockdown. (D) Raji cells treated with siRNA against Ezh2 were subjected to ChIP assays using anti-H3K27me3 antibody, followed by DNA extraction and real-time PCR to detect the DNA fragment of the Zp. (E to H) Raji cells treated with siRNA and TSA in the same manner were subjected to ChIP assays using anti-H3K27me3, anti-H3K9Ac, anti-H3K4me3, and anti-histone H3 antibodies, followed by DNA extraction and real-time PCR to detect the DNA fragment of the Zp.

specifically examine the effect of H4K20me3 methylation on the silencing of the BZLF1 gene, Suv420h1, the methyltransferase responsible for the modification, was knocked down by siRNA technology. When the transfection of si-Suv420h1 reduced the mRNA levels of the methyltransferase down to 36 or 31% of the control level (Fig. 10B), the 6.2- or 46.6-fold induction of BZLF1 mRNA was observed in the absence or presence of TSA, respectively (Fig. 10A). The remarkable induction of the BZLF1 gene by Suv420h1 knockdown and TSA (Fig. 10A) corresponded with the reduction of H4K20me3 levels and the elevation of active H3K9Ac and H3K4me3 markers (Fig. 10D to H). This indicates that the silencing of the BZLF1 promoter in Raji cells is brought about by histone H4K20me3 methylation as well. Therefore, histone acetylation, in addition to H4K20me3 demethylation, enhances promoter activity.

DISCUSSION

In this report, we document evidence that histone H3K27me3 and H4K20me3 play a crucial role in the suppression of the BZLF1 gene in Raji cells, mainly by using a small-molecule inhibitor of epigenetic modifications, DZNep. The pharmacological inhibitor reduced the levels of histone H3K27me3 and H4K20me3 markers, which coincides with BZLF1 induction when combined with an HDAC inhibitor, TSA.

Because DZNep exhibited potent inducing effects on BZLF1 gene transcription (Fig. 7), we also tested BIX01294, a specific inhibitor of G9a, the methyltransferase that is responsible for histone H3K9me2 methylation (30). However, the treatment of Raji cells or other EBV-positive cells with BIX01294 alone or in combination with TSA, DZNep, or 5-Aza did not increase BZLF1 expression at all or caused a very modest increase at most (Fig. 11). Although H3K9me2 methylation is ubiquitously detected in the EBV genome (Fig. 1E) (6, 12) and other herpesvirus genomes (18, 32, 52), the data imply that K3K9me2 does not play an important role in the suppression of BZLF1, at least in Raji cells. Further knockdown experiments are needed

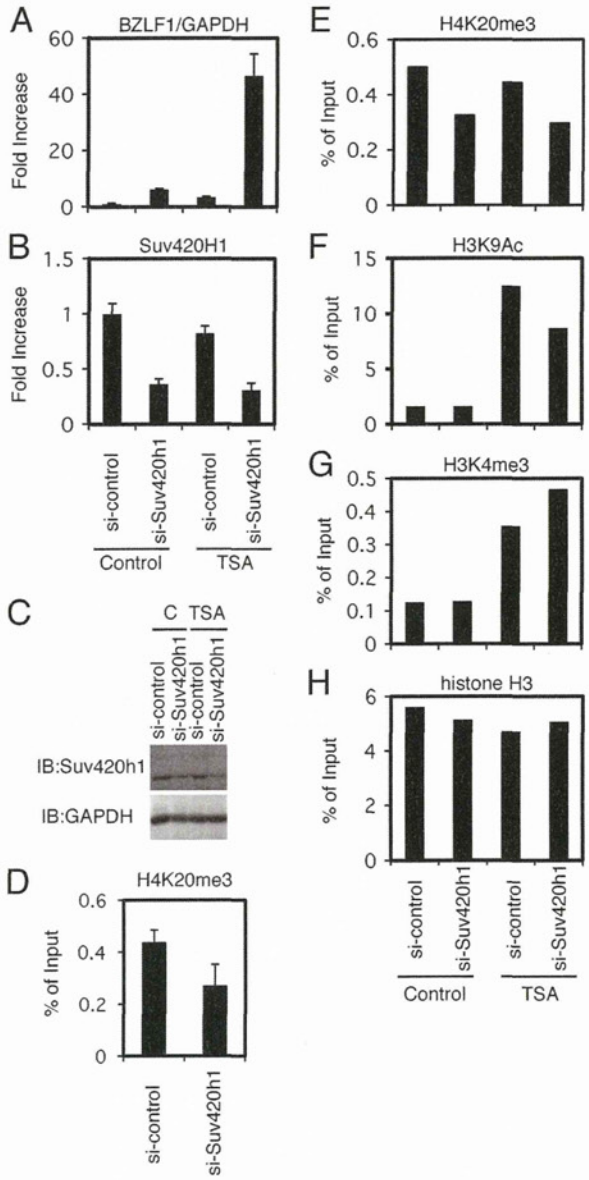

FIG 10 Knockdown of H4K20me3 methyltransferase Suv420h1. (A to C) Raji cells transfected with siRNA against Suv420h1 (si-Suv420h1) or a control siRNA (si-control) were cultured for 48 h and then treated with TSA (300 nM) or vehicle DMSO (Control) for an additional 24 h. Levels of BZLF1 (A) and Suv420h1 (B) mRNA were checked by real-time RT-PCR. (C) Levels of Suv420h1 protein were examined by immunoblotting. (D to H) Epigenetic status of the Zp after Suv420h1 knockdown. (D) Raji cells treated with siRNA against Suv420h1 were subjected to ChIP assays using anti-H4K20me3 antibody, followed by DNA extraction and real-time PCR to detect the DNA fragment of the Zp. (E to H) Raji cells treated with siRNA and TSA in the same manner were subjected to ChIP assays using anti-H4K20me3, anti-H3K9Ac, anti-H3K4me3, and anti-histone H3 antibodies, followed by DNA extraction and real-time PCR to detect the DNA fragment of the Zp.

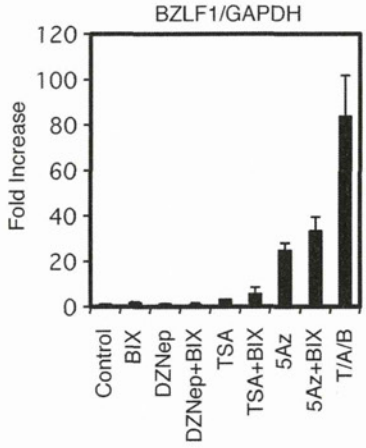

FIG 11 Effect of BIX01294, an inhibitor of G9a, a methyltransferase that is responsible for histone H3K9me2, on BZLF1 expression. Raji cells were treated with either vehicle (Control), 10 μM BIX01294 (BIX), 10 μM DZNep (DZ), 300 nM trichostatin A (TSA), 1 μM 5-aza-2′-deoxycytidine (5Az), or in combinations as indicated. As a positive control, Raji cells were treated with 20 ng/ml TPA, 1 μM A23187, and 5 mM sodium butyrate (T/A/B). For BIX01294, DZNep, or 5Az treatment, cells were exposed to the reagent daily for 3 days. Treatment with other chemicals were conducted for 24 h. Real-time RT-PCR was carried out as described in Materials and Methods. Levels of BZLF1 mRNAs were normalized to GAPDH mRNA levels and are shown as fold increases. Each bar represents the means and SD from three independent treatments.

to provide conclusive evidence of the involvement of H3K9 methylation in BZLF1 silencing.

Interestingly, whereas the treatment with TPA, A23187, and sodium butyrate did not alleviate repression markers, such as H3K9me2/me3, H3K27me3, or H4K20me3, at all (Fig. 1E to H), it did elicit the expression of BZLF1 (Fig. 7A). We suggest a hypothesis to explain this. It is known that multiple (50 to 100) copies of the episomal EBV genome are present per latent Raji cell (13, 56). If TPA-A23187-butyrate treatment induced reductions of such repressive histone methylations in only a few copies and allow the efficient expression of BZLF1 from the limited copies, the reduction of the repressive modifications must be hard to detect, because the histone methylations in most of the genome copies remain intact. Meanwhile, since the induction of active histone marks, like histone acetylation or H3K4me3 methylation, was clearly observed (Fig. 1C and D), such active marks may take place more broadly and efficiently among the viral copies.

A facultative repression marker, H3K27me3, is broadly found in EBV (Fig. 1G) (6, 12) and other herpesvirus (7, 18, 32, 52) genomes, and it functions to maintain latency (Fig. 7 and 9). We found here that H3K27me3, at least partly, functions in this regard by suppressing BZLF1 gene expression. On the other hand, another repression marker, H4K20me3, has not been implicated elsewhere in the suppression of herpesvirus gene expression.

The reduction of the H3K27me3 and H4K20me3 modifications by either siRNA or with an inhibitor caused the notable induction of the BZLF1 gene when treated with TSA (Fig. 7 and 10), indicating the importance of the methylations in silencing the BZLF1 promoter. However, we have to mention that the knockdown or use of inhibitors might cause unexpected influences on cellular genes, because histone H3K27me3- and H4K20me3-repressive marks are crucial regulators of many cellular genes. Thus, we cannot deny the possibility that the cellular gene(s) induced by the knockdown of the methylases or the inhibitor act on BZLF1 expression, and thus the enhanced BZLF1 expression we observe here might be a secondary effect of histone H3K27me3 or H4K20me3 downregulation.

EBV generally establishes latency in B cells in which BZLF1 expression is restricted by the epigenetic modification of histones but not CpG methylations (15). Similarly, lytic genes of HSV also

are suppressed primarily by repressive histone marks during latency in sensory neurons (4, 27, 54). On the other hand, it is estimated from HSV data (9, 46) that the herpesvirus DNA genome inside the nucleocapsid is not appreciably associated with histones, although the state of the EBV genome in viral particles has not been dissected yet. Upon infection, the herpesvirus genome becomes rapidly associated with cellular histones and nucleosomes, albeit irregularly (8, 25, 36, 46). Interestingly, upon the primary infection of EBV in naive B cells, the virus transcribes the BZLF1 gene (23, 55), although it cannot fully trigger the execution of the viral lytic replication cycle. These facts suggest that although the EBV genomic DNA in the incoming virus particle does not bear histones, it rapidly becomes incorporated into nucleosomes with active histone markers upon infection, which allows the expression of the BZLF1 gene at least for the first several days. Later, however, the expression is silenced by acquired repressive epigenetic modifications, such as histone H3K27me3 and H4K20me3, implying that the acquisition of repressive histone markers takes longer than that of active markers. Without such epigenetic silencing of BZLF1, the lytic replication of EBV causes the arrest of cell cycle progression (31) and eventual cell death. Besides those repressive histone modifications, however, other possible mechanisms, such as the absence of required activators, signal transductions, or the presence of repressors, can play a role in the restriction of the gene. In any case, the restriction of BZLF1 transcription in infected cells is a very crucial point for the life cycle of the virus and for the infinite proliferation capacity of infected cells.

It must be emphasized that the response of BZLF1 promoter activity to a certain epigenetic inhibitor depends largely on the cell type. To take one example, levels of BZLF1 mRNA in Akata cells were induced 53-fold by TSA treatment alone. Combination treatment of Akata cells with TSA plus DZNep did not further induce gene expression. Therefore, it is inferred that the BZLF1 gene in Akata cells is suppressed mostly by low acetylation levels of histones, even though the promoter in Akata was still modified by H3K27me3 (47) (Fig. 4) and H4K20me3 (Fig. 6). At the same time, the BZLF1 gene was hardly induced (1.0- and 3.3-fold) by TSA alone in B95-8 (Fig. 8) and Raji cells (Fig. 7A), respectively. The simultaneous use of the two inhibitors (TSA plus DZNep) induced the BZLF1 gene by 64-fold in Raji cells (Fig. 7A), but combined application (TSA plus DZNep) failed to increase the BZLF1 level at all in B95-8 cells (Fig. 8), suggesting the presence of other suppression mechanisms besides low acetylation, H3K27me3, and H4K20me3 in B95-8 cells. We speculate that this variety of silencing mechanisms means that BZLF1 gene expression somehow is suppressed in order to proliferate and achieve cancerous growth, but the mechanisms of the suppression do not matter, so long as it is not a constitutive, deep repression, such as CpG methylation (15, 28), which is generally irreversible.

The transcriptional activation of EBV regulatory genes by histone acetylation has been extensively reported elsewhere (11, 22), thus we focus here on H3K4me3, which has not been reported for the EBV BZLF1 promoter to our knowledge. Lines of evidence indicate the crucial role of histone H3K4me3 modification for the execution of the lytic replication process of HSV (21, 36, 45) and KSHV (18, 52) genomes. In Fig. 1C, of note, while histone H3K9 acetylation took place overall in the EBV genome in response to HDAC inhibitors, H3K4me3 occurred in a different manner: histones at Zp0 (−221 to +12) and Zp +500 were efficiently trimethylated at H3K4 by TPA-A23187-butyrate (Fig. 1D, Zp0 and Zp +500), but this was not true for other distal parts of the Zp (Fig. 1D, Zp-3000, Zp-2000, Zp-1200, and Zp-600). Because the Zp0 (−221 to +12) region coincides with the known minimal promoter sequence required for the reactivation of EBV from latency (3), this specificity may bring about the specific transcriptional activation of the BZLF1 gene by a particular transcription factor. We speculate that Zp-specific transcription factors, including Sp1, MEF2D, CREB, ATF, and/or XBP-1(s), recruit the H3K4 methyltransferase Set1 or MLL. We plan to further analyze the significance of this modification by using siRNA, inhibitor, and mutant EBV-BAC cells with mutations at arbitrary sites of the BZLF1 promoter, such as ZI or ZII (42), in future work.

Collectively, our results indicate that two histone modifications, H3K27me3 and H4K20me3, which are associated with the latent EBV BZLF1 promoter region, are at least partly involved in the maintenance of virus latency in Raji cells. With these silencing mechanisms, EBV restricts the expression of viral lytic genes and avoids surveillance by the host immune system. The involvement of two active markers, histone acetylation and H3K4 trimethylation, at the BZLF1 promoter is implicated in reactivation from viral latency. In addition, since the execution of the viral lytic program arrests cell cycle progression in EBV-infected cells (31), the induction of EBV lytic replication in EBV-positive cancers by epigenetic inhibitors, such as HDAC inhibitors, 5-Aza, and/or DZNep, may offer clinical applications as a type of oncolytic therapy in the future, especially when combined with antiviral drugs, such as ganciclovir (14).

ACKNOWLEDGMENTS

We thank W. Hammerschmidt, H. J. Delecluse, and N. Shimizu for providing the EBV-BAC system, HEK293 cells, and SNK6 cells, respectively. We also thank C. Noda and T. Gamano for technical assistance.

This work was supported by grants in aid for Scientific Research from the Ministry of Education, Science, Sports, Culture and Technology (no. 20390137 and 21022055 to T.T. and no. 20790362 and 22790448 to T.M.), the Ministry of Health, Labour and Welfare (to T.T.), and partly by the Uehara Memorial Research Fund (to T.T.), the Japan Leukaemia Research Fund, and the Yasuda Medical Foundation (to T.M.).

REFERENCES

1. **Amon W, Farrell PJ.** 2005. Reactivation of Epstein-Barr virus from latency. Rev. Med. Virol. **15**:149–156.
2. **Bhende PM, Dickerson SJ, Sun X, Feng WH, Kenney SC.** 2007. X-box-binding protein 1 activates lytic Epstein-Barr virus gene expression in combination with protein kinase D. J. Virol. **81**:7363–7370.
3. **Binne UK, Amon W, Farrell PJ.** 2002. Promoter sequences required for reactivation of Epstein-Barr virus from latency. J. Virol. **76**:10282–10289.
4. **Bloom DC, Giordani NV, Kwiatkowski DL.** 2010. Epigenetic regulation of latent HSV-1 gene expression. Biochim. Biophys. Acta **1799**:246–256.
5. **Cao R, et al.** 2002. Role of histone H3 lysine 27 methylation in Polycomb-group silencing. Science **298**:1039–1043.
6. **Chau CM, Lieberman PM.** 2004. Dynamic chromatin boundaries delineate a latency control region of Epstein-Barr virus. J. Virol. **78**:12308–12319.
7. **Cliffe AR, Garber DA, Knipe DM.** 2009. Transcription of the herpes simplex virus latency-associated transcript promotes the formation of facultative heterochromatin on lytic promoters. J. Virol. **83**:8182–8190.
8. **Cliffe AR, Knipe DM.** 2008. Herpes simplex virus ICP0 promotes both histone removal and acetylation on viral DNA during lytic infection. J. Virol. **82**:12030–12038.
9. **Cohen GH, et al.** 1980. Structural analysis of the capsid polypeptides of herpes simplex virus types 1 and 2. J. Virol. **34**:521–531.
10. **Countryman J, et al.** 2009. Stimulus duration and response time inde-

pendently influence the kinetics of lytic cycle reactivation of Epstein-Barr virus. J. Virol. **83**:10694–10709.
11. **Countryman JK, Gradoville L, Miller G.** 2008. Histone hyperacetylation occurs on promoters of lytic cycle regulatory genes in Epstein-Barr virus-infected cell lines which are refractory to disruption of latency by histone deacetylase inhibitors. J. Virol. **82**:4706–4719.
12. **Day L, et al.** 2007. Chromatin profiling of Epstein-Barr virus latency control region. J. Virol. **81**:6389–6401.
13. **Delecluse HJ, Bartnizke S, Hammerschmidt W, Bullerdiek J, Bornkamm GW.** 1993. Episomal and integrated copies of Epstein-Barr virus coexist in Burkitt lymphoma cell lines. J. Virol. **67**:1292–1299.
14. **Feng WH, Hong G, Delecluse HJ, Kenney SC.** 2004. Lytic induction therapy for Epstein-Barr virus-positive B-cell lymphomas. J. Virol. **78**: 1893–1902.
15. **Fernandez AF, et al.** 2009. The dynamic DNA methylomes of double-stranded DNA viruses associated with human cancer. Genome Res. **19**: 438–451.
16. **Flemington E, Speck SH.** 1990. Autoregulation of Epstein-Barr virus putative lytic switch gene BZLF1. J. Virol. **64**:1227–1232.
17. **Gradoville L, Kwa D, El-Guindy A, Miller G.** 2002. Protein kinase C-independent activation of the Epstein-Barr virus lytic cycle. J. Virol. **76**:5612–5626.
18. **Gunther T, Grundhoff A.** 2010. The epigenetic landscape of latent Kaposi sarcoma-associated herpesvirus genomes. PLoS Pathog. **6**:e1000935.
19. **Hagemeier SR, et al.** 2010. Sumoylation of the Epstein-Barr virus BZLF1 protein inhibits its transcriptional activity and is regulated by the virus-encoded protein kinase. J. Virol. **84**:4383–4394.
20. **Hatfull G, Bankier AT, Barrell BG, Farrell PJ.** 1988. Sequence analysis of Raji Epstein-Barr virus DNA. Virology **164**:334–340.
21. **Huang J, et al.** 2006. Trimethylation of histone H3 lysine 4 by Set1 in the lytic infection of human herpes simplex virus 1. J. Virol. **80**:5740–5746.
22. **Jenkins PJ, Binne UK, Farrell PJ.** 2000. Histone acetylation and reactivation of Epstein-Barr virus from latency. J. Virol. **74**:710–720.
23. **Kalla M, Schmeinck A, Bergbauer M, Pich D, Hammerschmidt W.** 2010. AP-1 homolog BZLF1 of Epstein-Barr virus has two essential functions dependent on the epigenetic state of the viral genome. Proc. Natl. Acad. Sci. U. S. A. **107**:850–855.
24. **Kennedy G, Sugden B.** 2003. EBNA-1, a bifunctional transcriptional activator. Mol. Cell. Biol. **23**:6901–6908.
25. **Kent JR, et al.** 2004. During lytic infection herpes simplex virus type 1 is associated with histones bearing modifications that correlate with active transcription. J. Virol. **78**:10178–10186.
26. **Kim YW, Kim A.** 2011. Characterization of histone H3K27 modifications in the beta-globin locus. Biochem. Biophys. Res. Commun. **405**:210–215.
27. **Knipe DM, Cliffe A.** 2008. Chromatin control of herpes simplex virus lytic and latent infection. Nat. Rev. Microbiol. **6**:211–221.
28. **Kondo Y.** 2009. Epigenetic cross-talk between DNA methylation and histone modifications in human cancers. Yonsei Med. J. **50**:455–463.
29. **Kondo Y, et al.** 2008. Gene silencing in cancer by histone H3 lysine 27 trimethylation independent of promoter DNA methylation. Nat. Genet. **40**:741–750.
30. **Kubicek S, et al.** 2007. Reversal of H3K9me2 by a small-molecule inhibitor for the G9a histone methyltransferase. Mol. Cell **25**:473–481.
31. **Kudoh A, et al.** 2003. Reactivation of lytic replication from B cells latently infected with Epstein-Barr virus occurs with high S-phase cyclin-dependent kinase activity while inhibiting cellular DNA replication. J. Virol. **77**:851–861.
32. **Kwiatkowski DL, Thompson HW, Bloom DC.** 2009. The polycomb group protein Bmi1 binds to the herpes simplex virus 1 latent genome and maintains repressive histone marks during latency. J. Virol. **83**:8173–8181.
33. **Liu P, Liu S, Speck SH.** 1998. Identification of a negative cis element within the ZII domain of the Epstein-Barr virus lytic switch BZLF1 gene promoter. J. Virol. **72**:8230–8239.
34. **Liu S, Borras AM, Liu P, Suske G, Speck SH.** 1997. Binding of the ubiquitous cellular transcription factors Sp1 and Sp3 to the ZI domains in the Epstein-Barr virus lytic switch BZLF1 gene promoter. Virology **228**: 11–18.
35. **Liu S, Liu P, Borras A, Chatila T, Speck SH.** 1997. Cyclosporin A-sensitive induction of the Epstein-Barr virus lytic switch is mediated via a novel pathway involving a MEF2 family member. EMBO J. **16**:143–153.
36. **Lu X, Triezenberg SJ.** 2010. Chromatin assembly on herpes simplex virus genomes during lytic infection. Biochim. Biophys. Acta **1799**:217–222.
37. **Luka J, Kallin B, Klein G.** 1979. Induction of the Epstein-Barr virus (EBV) cycle in latently infected cells by n-butyrate. Virology **94**:228–231.
38. **Miller G, El-Guindy A, Countryman J, Ye J, Gradoville L.** 2007. Lytic cycle switches of oncogenic human gammaherpesviruses. Adv. Cancer Res. **97**:81–109.
39. **Miranda TB, et al.** 2009. DZNep is a global histone methylation inhibitor that reactivates developmental genes not silenced by DNA methylation. Mol. Cancer Ther. **8**:1579–1588.
40. **Montalvo EA, Cottam M, Hill S, Wang YJ.** 1995. YY1 binds to and regulates cis-acting negative elements in the Epstein-Barr virus BZLF1 promoter. J. Virol. **69**:4158–4165.
41. **Murata T, et al.** 2010. Transcriptional repression by sumoylation of Epstein-Barr virus BZLF1 protein correlates with association of histone deacetylase. J. Biol. Chem. **285**:23925–23935.
42. **Murata T, et al.** 2011. Involvement of Jun dimerization protein 2 (JDP2) in the maintenance of Epstein-Barr virus latency. J. Biol. Chem. **286**: 22007–22016.
43. **Murata T, et al.** 2009. TORC2, a coactivator of cAMP-response element-binding protein, promotes Epstein-Barr virus reactivation from latency through interaction with viral BZLF1 protein. J. Biol. Chem. **284**:8033–8041.
44. **Nagata H, et al.** 2001. Characterization of novel natural killer (NK)-cell and gammadelta T-cell lines established from primary lesions of nasal T/NK-cell lymphomas associated with the Epstein-Barr virus. Blood **97**: 708–713.
45. **Narayanan A, Ruyechan WT, Kristie TM.** 2007. The coactivator host cell factor-1 mediates Set1 and MLL1 H3K4 trimethylation at herpesvirus immediate early promoters for initiation of infection. Proc. Natl. Acad. Sci. U. S. A. **104**:10835–10840.
46. **Oh J, Fraser NW.** 2008. Temporal association of the herpes simplex virus genome with histone proteins during a lytic infection. J. Virol. **82**:3530–3537.
47. **Ramasubramanyan S, Osborn K, Flower K, Sinclair AJ.** 2012. Dynamic chromatin environment of key lytic cycle regulatory regions of the Epstein-Barr virus genome. J. Virol. **86**:1809–1819.
48. **Ruf IK, Rawlins DR.** 1995. Identification and characterization of ZIIBC, a complex formed by cellular factors and the ZII site of the Epstein-Barr virus BZLF1 promoter. J. Virol. **69**:7648–7657.
49. **Schotta G, et al.** 2004. A silencing pathway to induce H3-K9 and H4-K20 trimethylation at constitutive heterochromatin. Genes Dev. **18**:1251–1262.
50. **Speck SH, Chatila T, Flemington E.** 1997. Reactivation of Epstein-Barr virus: regulation and function of the BZLF1 gene. Trends Microbiol. **5**:399–405.
51. **Tan J, et al.** 2007. Pharmacologic disruption of Polycomb-repressive complex 2-mediated gene repression selectively induces apoptosis in cancer cells. Genes Dev. **21**:1050–1063.
52. **Toth Z, et al.** 2010. Epigenetic analysis of KSHV latent and lytic genomes. PLoS Pathog. **6**:e1001013.
53. **Tsurumi T, Fujita M, Kudoh A.** 2005. Latent and lytic Epstein-Barr virus replication strategies. Rev. Med. Virol. **15**:3–15.
54. **Wang QY, et al.** 2005. Herpesviral latency-associated transcript gene promotes assembly of heterochromatin on viral lytic-gene promoters in latent infection. Proc. Natl. Acad. Sci. U. S. A. **102**:16055–16059.
55. **Wen W, et al.** 2007. Epstein-Barr virus BZLF1 gene, a switch from latency to lytic infection, is expressed as an immediate-early gene after primary infection of B lymphocytes. J. Virol. **81**:1037–1042.
56. **Yamamoto N, Bister K, zur Hausen H.** 1979. Retinoic acid inhibition of Epstein-Barr virus induction. Nature **278**:553–554.
57. **Ye J, Gradoville L, Daigle D, Miller G.** 2007. De novo protein synthesis is required for lytic cycle reactivation of Epstein-Barr virus, but not Kaposi's sarcoma-associated herpesvirus, in response to histone deacetylase inhibitors and protein kinase C agonists. J. Virol. **81**:9279–9291.
58. **Yu X, Wang Z, Mertz JE.** 2007. ZEB1 regulates the latent-lytic switch in infection by Epstein-Barr virus. PLoS Pathog. **3**:e194.

Cancer Gene Therapy (2012) 1 – 6

www.nature.com/cgt

ORIGINAL ARTICLE

HLA-restricted presentation of WT1 tumor antigen in B-lymphoblastoid cell lines established using a maxi-EBV system

T Kanda[1], T Ochi[2], H Fujiwara[2], M Yasukawa[2], S Okamoto[3], J Mineno[3], K Kuzushima[4,5] and T Tsurumi[1]

Lymphoblastoid cell lines (LCLs), which are established by *in vitro* infection of peripheral B-lymphocytes with Epstein–Barr virus (EBV), are effective antigen-presenting cells. However, the ability of LCLs to present transduced tumor antigens has not yet been evaluated in detail. We report a single-step strategy utilizing a recombinant EBV (maxi-EBV) to convert B-lymphocytes from any individuals into indefinitely growing LCLs expressing a transgene of interest. The strategy was successfully used to establish LCLs expressing Wilms' tumor gene 1 (WT1) tumor antigen (WT1-LCLs), which is an attractive target for cancer immunotherapy. The established WT1-LCLs expressed more abundant WT1 protein than K562 leukemic cells, which are known to overexpress WT1. A WT1-specific cytotoxic T lymphocyte line efficiently lysed the WT1-LCL in a human leukocyte antigen-restricted manner, but poorly lysed control LCL not expressing WT1. These results indicate that the transduced WT1 antigen is processed and presented on the WT1-LCL. This experimental strategy can be applied to establish LCLs expressing other tumor antigens and will find a broad range of applications in the field of cancer immunotherapy.

Cancer Gene Therapy advance online publication, 22 June 2012; doi:10.1038/cgt.2012.34

Keywords: Wilms' tumor gene; Epstein–Barr virus; bacterial artificial chromosome; lymphoblastoid cell line

INTRODUCTION

Epstein–Barr virus (EBV) is a human gammaherpesvirus that can infect primary B-lymphocytes and transform them into continuously growing lymphoblastoid cell lines (LCLs) *in vitro*.[1] LCLs are valuable tools in immunological studies and can easily be established by infecting peripheral lymphocytes of any individuals with a prototype strain of EBV, B95-8.[2] The majority of cells in the LCLs are latently infected and express a set of EBV latent genes, some of which are responsible for EBV-induced B-cell transformation.[1] In addition, a minority of cells in the LCLs spontaneously enter virus productive cycle and express several lytic genes, although they produce few infectious progeny. As a result, LCLs present immunogenic peptides derived from EBV latent and lytic gene products complexed with major human leukocyte antigen (HLA) molecules on the cell surface.[3,4] Furthermore, as the process of EBV-induced B-cell immortalization mimics physiological B-cell proliferation, LCLs express various cell surface markers that are preferentially expressed on activated B cells. These markers on LCLs include B-cell activation markers (such as CD23 and CD30), cell-adhesion molecules (such as LFA1, LFA3 and ICAM1) and T-cell costimulatory molecules (such as CD80 and CD86).[5] Owing to the expression of these surface molecules, LCLs, like activated B cells, could serve as good antigen-presenting cells. Antigen presentation of EBV-derived peptides by LCLs is demonstrated by *ex vivo* expansion of EBV-specific cytotoxic T lymphocytes (CTLs) following co-cultivation of peripheral blood mononuclear cells (PBMCs) with autologous LCLs.[6,7] Similarly, antigen presentation by EBV-infected B cells also occurs *in vivo*, leading to the induction of EBV-specific CTL in humans.[8] Such EBV-specific CTL are essential in maintaining control of latently infected cells *in vivo*, although they are unable to eliminate EBV from the body.[9]

Owing to their ease of establishment and cultivation, LCLs are widely used as antigen-presenting cells for a range of foreign antigens. For example, LCLs can be loaded with antigenic peptides, which bind to HLA molecules and are presented on the cell surface.[10] Alternatively, foreign antigens can be expressed in LCLs by infecting LCLs with recombinant retroviruses[11] or adenoviruses expressing foreign antigens.[12]

To simplify the establishment of LCLs presenting foreign antigen, a single-step strategy was developed by utilizing so-called 'mini-EBVs'.[13] Mini-EBV (71 kb in size) contains minimal viral genes that are essential for B-cell immortalization,[14,15] whereas maxi-EBV (175 kb in size) contains an entire EBV genome.[16] In mini-EBV system, a transgene of interest was inserted into a mini-EBV plasmid, and the resultant plasmid was then transfected into a EBV packaging cell line to produce virion-packaged mini-EBV.[13] Infecting B-lymphocytes with virion-packaged mini-EBVs *ex vivo* results in the establishment of LCLs designated as 'mini-LCLs'. Although this strategy can theoretically be applied to various antigens, it has not been applied to tumor-associated antigens, with the only exception of mini-LCLs expressing Mucin (MUC1).[17] Importantly, HLA-restricted presentation of tumor-associated antigens in mini-LCLs has never been examined to date.

[1]Division of Virology, Aichi Cancer Center Research Institute, 1-1 Kanokoden, Chikusa-ku, Nagoya, Aichi, Japan; [2]Department of Bioregulatory Medicine, Ehime University, Graduate School of Medicine, Shitsukawa, Toon, Ehime, Japan; [3]Center for Cell and Gene Therapy, Takara Bio, 3-4-1 Seta, Ohtsu, Shiga, Japan; [4]Disivion of Immunology, Aichi Cancer Center Research Institute, 1-1 Kanokoden, Chikusa-ku, Nagoya, Aichi, Japan and [5]Department of Cellular Oncology, Nagoya University Graduate School of Medicine, Nagoya, 65 Tsurumai-cho, Showa-ku, Nagoya, Japan. Correspondence: Dr T Kanda, Division of Virology, Aichi Cancer Center Research Institute, 1-1 Kanokoden, Chikusa-ku, Nagoya, Aichi 464-8681, Japan.
E-mail: tkanda@aichi-cc.jp
Received 14 November 2011; revised 8 May 2012; accepted 23 May 2012

The Wilms' tumor gene 1, WT1, was first identified in a mutated form in the childhood neoplasm, Wilms' tumor,[18] and at that time, wild-type WT1 was categorized as a tumor-suppressor gene. Expression of the WT1 gene is restricted to a limited number of normal tissues including fetal kidney, hematopoietic precursors, ovary, testis and spleen.[19] Later, high levels of WT1 expression in most human acute leukemias[20] and in a variety of malignant solid tumors[21] were reported. The restricted expression of WT1 in normal adult tissues, and its overexpression in a broad spectrum of malignancies, has led to reconsideration of WT1 as a tumor-associated antigen. Thus, WT1 is now recognized as an attractive target for cancer immunotherapy. WT1 peptide-loaded LCLs can efficiently stimulate WT1-specific CTL *in vitro* and *in vivo*.[10] We envisioned that expressing whole WT1 protein in LCLs would enable the presentation of multiple WT1 epitopes on the surface of LCLs.

We previously reported that a bacterial artificial chromosome (BAC) clone encompassing the entire EBV (Akata strain) genome can be utilized as a convenient vector for transgene expression in LCLs.[22] We recently established a new BAC clone of B95-8 strain of EBV and improved the method to produce pure recombinant viruses with higher transforming titers.[23] The newly obtained BAC clone (174-kb BAC) is similar to a precedent called 'maxi-EBV',[16] but it is unique in that it stably maintains a viral repetitive sequence (designated as Family of Repeats) and enables production of recombinant EBVs with excellent transgene expression.[23] We applied this novel 'maxi-EBV system' to produce a recombinant EBV expressing WT1. Here, we demonstrate that the recombinant virus enables us to readily establish LCLs expressing WT1, which is processed and presented to HLA-A24-restricted WT1-specific CTLs. The results highlight the utility of this novel maxi-EBV system.

MATERIALS AND METHODS

Cell lines

HEK293 cells[24] and established LCLs were maintained in RPMI 1640 medium (Sigma-Aldrich Fine Chemicals, St Louis, MO) supplemented with 10% fetal bovine serum.

Plasmids

A plasmid double-I-PpoI was constructed as described previously.[22] A kanamycin-resistance gene derived from PUC4K was inserted into the *Eco*RI site of double-I-PpoI to make double-I-PpoI-km. An mCherry gene or a complementary DNA clone of WT1 (variant D)[25] were cloned into the *Hin*cII site of double-I-PpoI to make double-I-PpoI-mCherry or double-I-PpoI-WT1, respectively.

Insertion of transgenes into BAC-cloned B95-8-strain EBV genome

Large quantities of BAC clone DNAs were prepared from each 250 ml bacterial culture using a Nucleobond BAC100 kit (Macherey-Nagel, Duren, Germany).

For making EBV-BAC-I-PpoI, a plasmid double-I-PpoI-km (kanamycin-resistant gene flanked with two I-PpoI sites) was PCR amplified using a pair of 70-mer oligonucleotides, which carry a 50 nucleotide region homologous to the target region in the 174-kb BAC. A linear PCR product was used as a targeting construct. Recombinogenic engineering of BAC clones was performed in electrocompetent DH10B cells using standard Red/ET protocols.[26] The kanamycin-resistance marker gene was removed by digesting the BAC clone with I-PpoI, followed by self-ligation.

EBV-BAC-mCherry and EBV-BAC-WT1 were constructed by inserting the I-PpoI fragment of either double-I-PpoI-mCherry or double-I-PpoI-WT1 into the unique I-PpoI site of EBV-BAC-I-PpoI via *in vitro* ligation as described.[22]

Recombinant virus production

HEK293 cells (4×10^5 cells) were plated in six-well tissue culture dishes and transfected with BAC clone DNA (1 μg, prepared with the Nucleobond BAC100 kit) using lipofectamine 2000 (Invitrogen, Carlsbad, CA, USA). Two days after transfection, the transfected cells were re-plated at a density of 4000 cells per well in 96-well tissue culture plates in medium containing 150 μg of hygromycin per ml. Hygromycin-resistant cell clones with bright green fluorescent protein (GFP) were grown, and clones that were highly competent for entering lytic replication after expressing BZLF1 (a viral switch gene required for progeny virus production) were selected.

HEK293 cells carrying recombinant EBV episomes were transfected with BZLF1 expression vector or with BZLF1 and gp110 expression vectors using lipofectamine 2000. Culture supernatants containing recombinant viruses were harvested at 3 days post-transfection and filtered through 0.45-μm pore-size filter.

B-cell transformation

Blood samples were obtained from normal donors (A24/, A26/33 and A24/11) according to protocols approved by the institutional review board of Aichi Cancer Center, Nagoya, Japan. PBMCs were infected with serially diluted (10^{-1} to 10^{-3}) culture supernatants containing recombinant EBV-BAC-WT1 viruses and plated at 1×10^5 cells per well in 96-well tissue culture plates in medium containing cyclosporine A (500 ng ml^{-1}). Half of the culture medium was replaced with fresh medium containing cyclosporine A every 5 days. The established LCLs were expanded in culture medium containing hygromycin (50 μg ml^{-1}).

For checking GFP and mCherry expression, cells were fixed in phosphate-buffered saline (without calcium and magnesium) containing 0.5% paraformaldehyde. Fluorescence was measured using a FACSCalibur (Becton Dickinson, Franklin Lakes, NJ, USA). The green (GFP) and red (mCherry) emissions from each cell line were measured using FL1 and FL2 channels, respectively, without color compensation. Data analysis was done using CellQuest software (Becton Dickinson).

Western blot analysis

Whole cell extracts were prepared by lysing cells with sodium dodecyl sulfate lysis buffer (3% sodium dodecyl sulfate, 10% glycerol, 125 mM Tris-Cl pH 6.7, 6% urea) at a concentration of 1×10^7 per ml. Aliquots of whole cell extracts were analyzed by sodium dodecyl sulfate-7% polyacrylamide gel electrophoresis. Western blot analysis was performed according to standard ECL protocols. Anti-WT1 rabbit polyclonal antibody (1:500 dilution; C19, Santa Cruz, Santa Cruz, CA, USA) was used as a primary antibody, and a horseradish peroxidase-conjugated anti-rabbit immunoglobulin G (1:2000; GE Healthcare, Piscataway, NJ, USA) was used as a secondary antibody.

Cytotoxicity assays

Cytotoxic assays were performed as described previously.[27] Briefly, 1×10^4 ^{51}Cr (Na_2 $^{51}CrO_4$)-labeled target cells in 100 μl RPMI 1640 medium supplemented with 10% fetal bovine serum (assay medium) were seeded into a 96-well round-bottom microtiter plate and incubated with and without a synthetic 9-mer peptide CMTWNQMNL (residues 235–243) for 2 h. A T-cell line retrovirally transduced with HLA-A24-restricted WT1-specific T cell receptor (TCR) α/β genes (WT1-TCR-CTL)[28] was used as effector cells in the assays. Varying numbers of WT1-TCR-CTL suspended in 100 μl assay medium were added to the well, and the plate was incubated at 37 °C for 4 h. After the incubation, 100 μl supernatant was collected from each well, and its radioactivity was counted on a γ-scintillation counter. The percentage of specific lysis was calculated as follows: (counts per minute (c.p.m.) experimental release−c.p.m. spontaneous release)/(c.p.m. maximal release−c.p.m. spontaneous release) × 100.

RESULTS

Production of recombinant EBVs with various transgenes

We recently obtained a novel EBV(B95-8 strain)-BAC clone, designated as the 174-kb BAC.[23] The 174-kb BAC contained a GFP

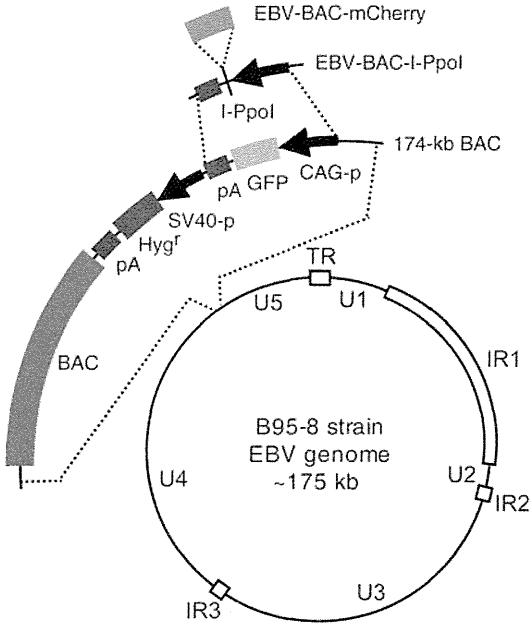

Figure 1. A schematic representation of the Epstein–Barr virus (EBV)-bacterial artificial chromosome (BAC) clone (maxi-EBV), designated as 174-kb BAC, and its derivatives. Unique regions (U1 through U5), internal repeat regions (IR1, IR2 and IR3) and the terminal repeats (TRs) of the EBV genome (B95-8 strain) are indicated. The 174-kb BAC has a green fluorescent protein (GFP) gene driven by CAG promoter (CAG-p), a hygromycin-resistance gene (Hyg^r) driven by SV40 promoter (SV40-p), and a BAC vector sequence, inserted between U4 and U5 regions of the B95-8 EBV genome. The creation of I-PpoI site and subsequent insertion of an mCherry gene into the I-PpoI site are illustrated.

transgene driven by the CAG promoter (a chimeric promoter consisting of cytomegalovirus-immediate early, chicken β-actin, and rabbit β-globin promoters) (Figure 1), which works efficiently in a broad spectrum of cells.[29] The 174-kb BAC clone DNA was stably transfected into HEK293 cells to obtain virus-producing cells, and recombinant EBV derived from the 174-kb BAC exhibited high B-cell transformation efficiency. PBMC from healthy donors were infected with the recombinant EBV of the 174-kb BAC. GFP expression in the transformed lymphocytes became apparent starting at 3 days post-infection. Multiple lines of LCL were established within 1 month after infection, and were cultured with hygromycin selection to minimize the loss of EBV episomes. In most LCL cultures, >90% of the cells were GFP-positive (Figure 2). Thus, a recombinant EBV derived from the 174-kb BAC appeared to be useful for expressing transgenes in LCLs derived from a range of different individuals.

We set out to modify the 174-kb BAC clone so that we could easily replace the GFP with other transgenes. We introduced a recognition sequence of an intron-encoded endonuclease I-PpoI into the 174-kb BAC (Figure 1). The recognition sequence of I-PpoI is longer than 15 bp[30] and is absent from the parental 174-kb BAC. Thus, the artificially created I-PpoI site is a unique site within the modified BAC clone, and enables the insertion of complementary DNA cassettes by simple *in vitro* ligation.[22]

As a proof of concept, we used the strategy to generate a recombinant EBV genome with a red fluorescent protein (mCherry) transgene.[31] An mCherry gene was inserted into the created I-PpoI site to obtain EBV-BAC-mCherry (Figure 1). The recombinant EBV expressing mCherry was produced using a similar protocol to that used for producing the 174-kb BAC virus, and peripheral B-lymphocytes were infected with the recombinant virus expressing the mCherry transgene. Multiple lines of LCL

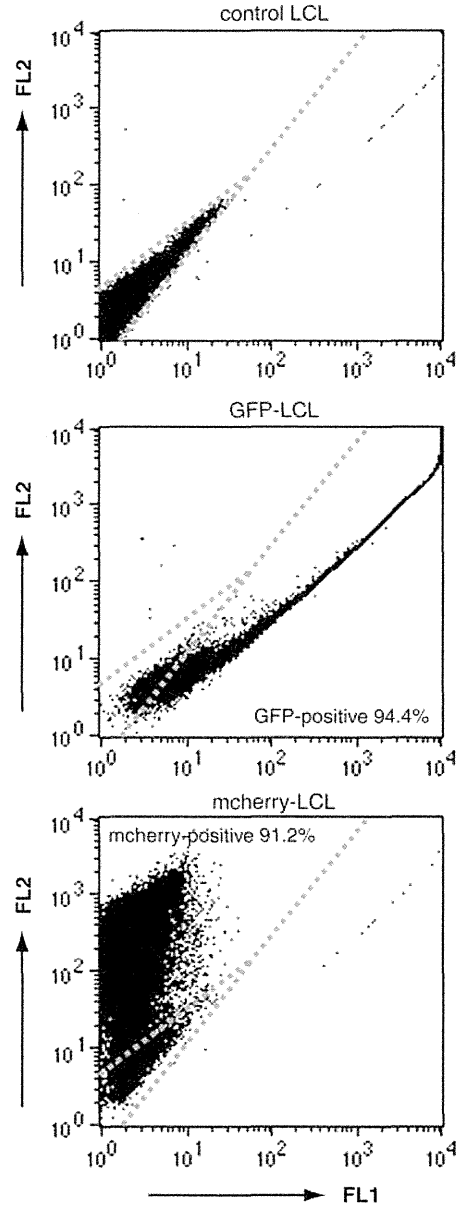

Figure 2. Recombinant Epstein–Barr virus (EBV) can be used to establish lymphoblastoid cell lines (LCLs) expressing various transgenes. A control LCL (established using the B95-8 strain of EBV), a green fluorescent protein (GFP)-LCL, and an mCherry-LCL were analyzed by fluorescence-activated cell sorting (FACS) using the FL1 and FL2 channels. GFP-expressing cells were identified by the shift of fluorescence intensity in the FL1 channel, whereas mCherry-expressing cells were identified by the shift of fluorescence in the FL2 channel. Numbers represent the percentage of GFP- or mCherry-expressing cells.

expressing mCherry were established (mCherry-LCLs), with most cultures containing >90% mCherry-positive cells (Figure 2). These results indicate that it should be feasible to establish LCLs expressing any kind of antigen, unless the antigen impairs the growth of LCLs.

Establishing LCLs expressing WT1 antigen

We then proceeded to apply the strategy to establish LCLs expressing the WT1 tumor antigen. A WT1 complementary DNA

(variant D)[25] was inserted into the unique I-PpoI site of the parental BAC clone to construct EBV-BAC-WT1, and virus-producing cells were obtained by stable transfection of the EBV-BAC-WT1 into HEK293 cells.

PBMC from three healthy donors (donor 1, HLA A24/; donor 2, HLA A26/33; and donor 3, A24/11) were infected with the recombinant EBV derived from EBV-BAC-WT1 to establish LCLs expressing WT1 (WT1-LCLs). PBMCs from the same donors were also infected with the parental 174-kb BAC virus to establish GFP-LCLs. Multiple WT1-LCLs and GFP-LCLs were obtained from the lymphocytes of three donors. The expression of WT1 in the WT1-LCLs was examined by western analysis, along with a human leukemic cell line K562 as a positive control for WT1 expression. A representative result obtained using cell extracts from two independent lines of GFP-LCL and WT-LCL (both derived from donor 1) is shown in Figure 3a. WT1-LCLs expressed substantial amounts of the protein, whereas GFP-LCLs did not express any detectable WT1 protein. The expression of WT1 in the WT1-LCLs was significantly higher than in K562 cells (Figure 3a). WT1-LCLs derived from the donor 2 and 3 also expressed substantial amounts of WT1 (Figure 3b), clearly demonstrating that this experimental strategy can be applied to any individual.

We utilized immunofluorescence to measure the frequency of WT1-positive cells in the WT1-LCLs. The majority of WT1-LCL cells expressed WT1 (Figure 3c), although the staining intensity was heterogeneous among the cells. Such heterogeneity is characteristic of transgene expression from episomally maintained EBV genomes, as varied copies of episomes are maintained in individual cells. A higher magnification image obtained by a confocal microscopy revealed that WT1 localized in the nuclei of the WT1-LCLs and constituted several densely stained nuclear dots (Figure 3d).

WT1 antigen presentation in WT1-LCLs

Although WT1 is a nuclear protein, it is processed and presented as a short peptide to relevant CTLs.[32] We examined whether WT1 was processed and presented on the WT1-LCLs as evidenced by specific lysis by WT1-specific CTLs. To this end, we utilized a T-cell line expressing HLA-A24-restricted WT1-specific TCR α/β chains (WT1-TCR-CTL)[28] as effector cells in CTL assays. A set of

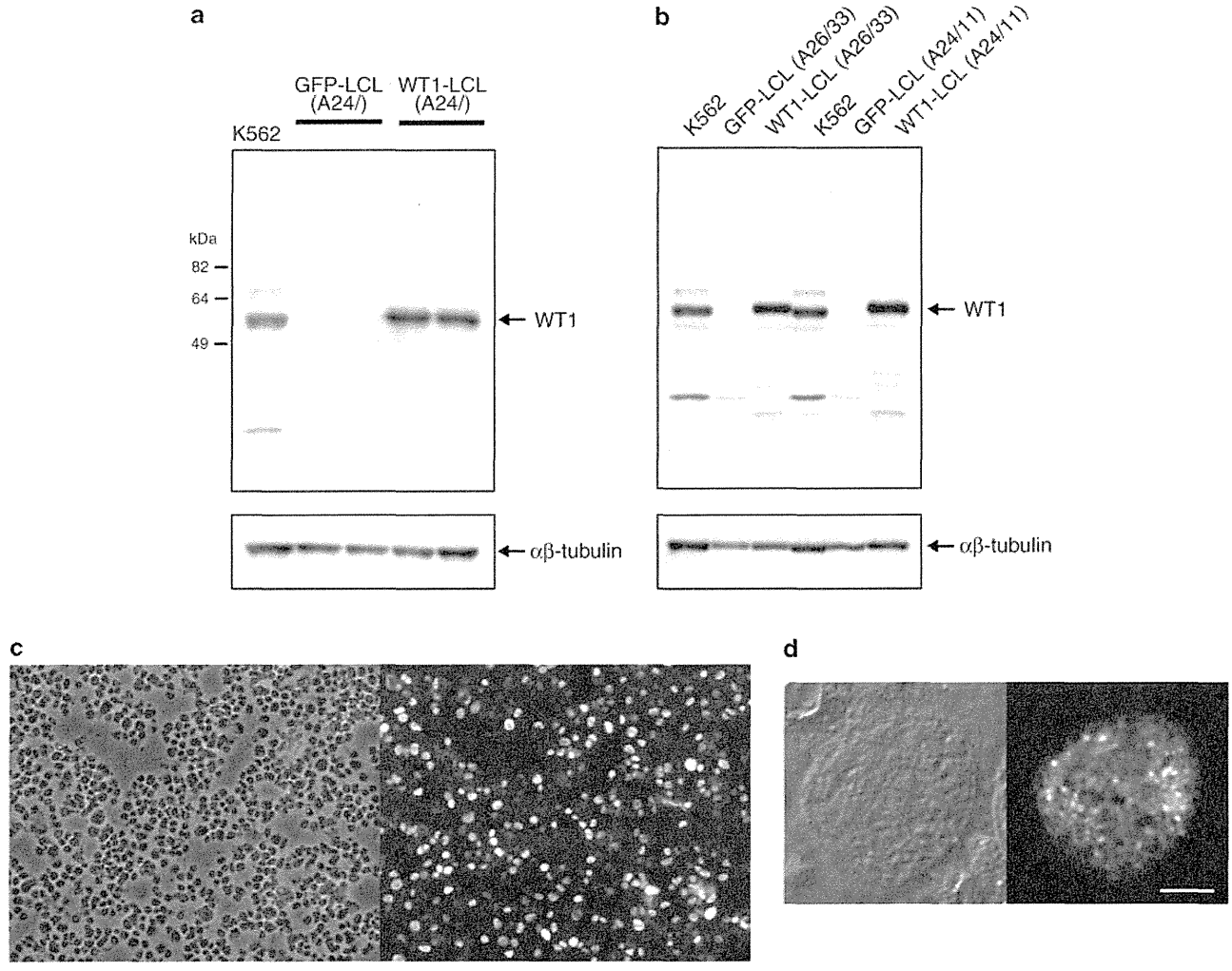

Figure 3. (**a**) The expression of Wilms' tumor gene 1 (WT1) in WT1-lymphoblastoid cell lines (LCLs). Whole cell extracts from K562 cells, two independent lines of green fluorescent protein (GFP)-LCLs (derived from donor 1) and of WT1-LCLs (derived from the same donor) were analyzed by western blot analysis using WT1-specific antibody as a primary antibody. The expression of α/β-tubulin was measured as an internal control. (**b**) GFP-LCLs and WT1-LCLs, derived from donor 2 (A26/33) and donor 3 (A24/11), were analyzed by western blot analysis as in (**a**). (**c**) The expression of WT1 in a WT1-LCL (derived from donor 1) was assessed by immunofluorescence using the same antibody as in (**a**). A phase contrast image (top panel) and an epifluorescence image (bottom panel) are shown. (**d**) A confocal microscopic image with a higher magnification demonstrates the intranuclear localization of WT1 protein in the WT1-LCL. The scale bar is 5 μm.

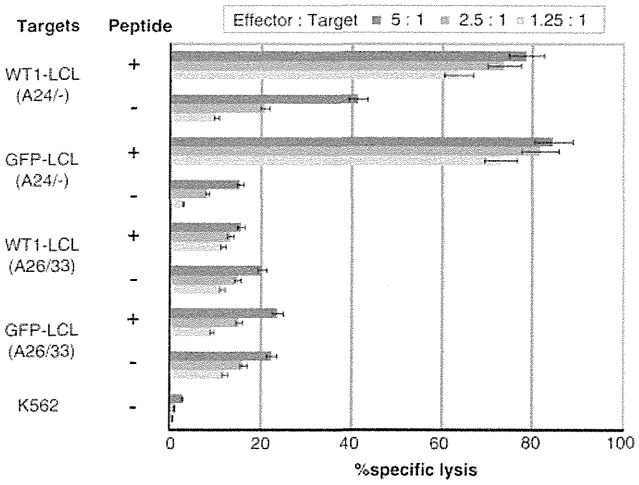

Figure 4. Cytotoxicity of Wilms' tumor gene 1 (WT1)- T cell receptor (TCR)-cytotoxic T lymphocyte (CTL) against various target cells. Two sets of WT1-lymphoblastoid cell line (LCL) and green fluorescent protein (GFP)-LCL, either from donor 1 (A24/) or donor 2 (A26/33), were used as targets in a cytotoxicity assay. Where indicated, cells were loaded with WT1-derived peptide (CMTWNQMNL). Note that WT1-LCL(A24/) was specifically lysed by WT1-TCR-CTL, whereas GFP-LCL(A24/) was barely lysed by the same CTL.

WT1-LCL(A24/) and GFP-LCL(A24/), both derived from the donor 1 lymphocytes, were used as target cells in CTL assays, in the presence or absence of WT1-specific peptide pulsing. When LCLs were pulsed with the peptide, both the WT1-LCL(A24/) and the GFP-LCL(A24/) were efficiently lysed by the WT1-TCR-CTL (Figure 3a). In the absence of the peptide, the GFP-LCL(A24/) was poorly lysed by the WT1-TCR-CTL. By contrast, the WT1-LCL (A24/) was efficiently lysed by WT1-TCR-CTL (>40% specific lysis at effector: target ratio of 5:1) (Figure 4).

We then examined whether the observed killing by WT1-TCR-CTL was HLA-A24 restricted. For this purpose, a set of WT1-LCL(A26/33) and a GFP-LCL(A26/33), both derived from the donor 2 lymphocytes, were used in the CTL assay. Both WT1-LCL(A26/33) and the control LCL(A26/33) were not lysed by WT1-TCR-CTL, regardless of WT1-peptide pulsing. These results indicate that the WT1-derived peptide was presented on the WT1-LCL in an HLA-restricted manner. Therefore, we conclude that the WT1-LCLs serve as target cells of WT1-specific CTLs, and that our experimental strategy provides useful research tools in the field of cancer immunotherapy.

DISCUSSION

EBV-LCLs are regarded as convenient tools for a variety of immunological studies, as they can be easily established from peripheral blood of any individual, and it is relatively easy to obtain large quantities without the aid of exogenous cytokines. We demonstrated here that a novel 'maxi-EBV' with a WT1 transgene can be used to readily convert resting B-lymphocytes to WT1-expressing LCLs *ex vivo*.

A strategy to establish LCLs with transgene expression requires two successive procedures: first, establishing LCLs using the B95-8 strain of EBV and, second, transducing the established LCLs by plasmid transfection or recombinant virus infection (either retrovirus or adenovirus).[11,12] A previously reported mini-EBV system is an attractive alternative, as one can convert PBMC to transgene-expressing LCLs via just single infection of mini-EBV.[13] On the other hand, production of mini-EBVs requires EBV packaging cell lines, and, as a result, recombinational events between mini-EBVs and helper virus genomes can be problematic. The advantage of maxi-EBV system is its simplicity; once HEK293 cells harboring maxi-EBVs are established, maxi-EBVs are stably maintained in the cells and can repeatedly produce viruses. A maxi-EBV lacking viral transactivator BZLF1, a critical switch gene for progeny virus production, was previously reported,[33] and similar modification is expected to solve the safety issue of our maxi-EBV system in the future.

We, for the first time, quantitatively evaluated the expression level of various transgenes in the established LCLs. Fluorescence-activated cell sorting, immunofluorescence and western analyses demonstrated the excellent levels of transgene expression. Latently infected maxi-EBV are maintained as episomes and do not integrate into host chromosomes. Therefore, the WT1 transgene is essentially free from position effects associated with chromosomal integration.[34] As a result, high-level expression of WT1 protein can be maintained during proliferation of WT1-LCLs.

This strategy is applicable for individuals with any HLA type. Our data clearly indicate that WT1 is processed and presented as an HLA-binding peptide on WT1-LCLs. Although we examined only one HLA class I-associated epitope, it is highly likely that others, including epitopes complexed with HLA class II, are also presented on WT1-LCLs. In addition, the strategy can be applied for any other tumor antigens, unless they impair the growth of LCLs. LCLs expressing tumor antigens can be ideal target cells of tumor antigen-specific CTLs.

On the other hand, using WT1-LCLs for *ex vivo* CTL induction can be problematic. Our attempts to utilize WT1-LCLs for *ex vivo* expansion of WT1-specific CTL were hampered by several technical limitations. For example, as the blood donors were EBV-seropositive and their PBMC contained pre-existing EBV-specific memory T cells, the expansion of EBV-specific CTLs became predominant after co-cultivation with autologous WT1-LCLs. We also tested a WT1-LCL derived from EBV-seronegative donor (donor 3, see Figure 3b) for *ex vivo* WT1-specific CTL induction, expecting that the lack of EBV-specific memory T cells favor the induction of WT1-specific CTLs. However, induction of WT1-specific CTL again failed (data not shown). Clearly, we need to test alternative experimental strategies. One possibility is to utilize WT1 peptide-pulsed dendritic cells for initial priming before the co-cultivation with WT1-LCLs. Another possibility is to utilize truncated WT1 protein instead of the full-length WT1 for transgene expression. This may augment immunogenicity because previous studies demonstrated that human WT1 truncated at the carboxy-terminal end localizes to the cytoplasm and is more immunogenic than its full-length counterpart.[35,36]

In summary, we developed a novel maxi-EBV strategy to establish LCLs potentially capable of expressing various tumor antigens as transgenes. These LCLs expressing tumor antigens can be used as target cells in CTL assay, providing useful research tools in the field of cancer immunotherapy. The utility of these LCLs for *ex vivo* CTL expansion is currently unclear, and should be pursued in the future.

CONFLICT OF INTEREST

The authors declare no conflict of interest.

ACKNOWLEDGEMENTS

We thank K Semba (Waseda University) for providing us with WT1 complementary DNA plasmids. This work was supported in part by a Grant-in-Aid for Scientific Research from the Ministry of Education, Culture, Sports, Science, and Technology, Japan (TK and TT), by a Grant-in-Aid for Scientific Research the Ministry of Health Labour and Welfare (TK and KK), by a grant of NOASTEC (Northern Advancement Center for Science and Technology) (TK), and by a grant from the Naito Foundation (TK).

REFERENCES

1 Kieff E, Rikinson AB. Epstein-Barr virus and its replication. In: Knipe M, Howley PM, (eds). *Fields Virology*, Vol 2. 4th edn. Lippincott Williams and Wilkins: Philadelphia, 2001, pp 2511–2573.
2 Miller G, Lipman M. Release of infectious Epstein-Barr virus by transformed marmoset leukocytes. *Proc Natl Acad Sci USA* 1973; **70**: 190–194.
3 Kuzushima K, Hayashi N, Kudoh A, Akatsuka Y, Tsujimura K, Morishima Y *et al.* Tetramer-assisted identification and characterization of epitopes recognized by HLA A*2402-restricted Epstein-Barr virus-specific CD8+ T cells. *Blood* 2003; **101**: 1460–1468.
4 Rickinson AB, Moss DJ. Human cytotoxic T lymphocyte responses to Epstein-Barr virus infection. *Annu Rev Immunol* 1997; **15**: 405–431.
5 Young LS, Rickinson AB. Epstein-Barr virus: 40 years on. *Nat Rev Cancer* 2004; **4**: 757–768.
6 Rickinson AB, Moss DJ, Allen DJ, Wallace LE, Rowe M, Epstein MA. Reactivation of Epstein-Barr virus-specific cytotoxic T cells by *in vitro* stimulation with the autologous lymphoblastoid cell line. *Int J Cancer* 1981; **27**: 593–601.
7 Rooney CM, Smith CA, Ng CY, Loftin S, Li C, Krance RA *et al.* Use of gene-modified virus-specific T lymphocytes to control Epstein-Barr-virus-related lymphoproliferation. *Lancet* 1995; **345**: 9–13.
8 Moss DJ, Rickinson AB, Pope JH. Long-term T-cell-mediated immunity to Epstein-Barr virus in man. I. Complete regression of virus-induced transformation in cultures of seropositive donor leukocytes. *Int J Cancer* 1978; **22**: 662–668.
9 Rickinson AB, Kieff E. Epstein-Barr virus. In: Knipe M, Howley PM, (eds). *Fields Virology*, Vol 2. 4th edn. Lippincott Williams and Wilkins: Philadelphia, 2001, pp 2575–2627.
10 Doubrovina ES, Doubrovin MM, Lee S, Shieh J-H, Heller G, Pamer E *et al. In vitro* stimulation with WT1 peptide-loaded Epstein-Barr virus-positive B cells elicits high frequencies of WT1 peptide-specific T cells with *in vitro* and *in vivo* tumoricidal activity. *Clin Cancer Res* 2004; **10**: 7207–7219.
11 Sun Q, Pollok KE, Burton RL, Dai LJ, Britt W, Emanuel DJ *et al.* Simultaneous *ex vivo* expansion of cytomegalovirus and Epstein-Barr virus-specific cytotoxic T lymphocytes using B-lymphoblastoid cell lines expressing cytomegalovirus pp65. *Blood* 1999; **94**: 3242–3250.
12 Leen AM, Myers GD, Sili U, Huls MH, Weiss H, Leung KS *et al.* Monoculture-derived T lymphocytes specific for multiple viruses expand and produce clinically relevant effects in immunocompromised individuals. *Nat Med* 2006; **12**: 1160–1166.
13 Moosmann A, Khan N, Cobbold M, Zentz C, Delecluse HJ, Hollweck G *et al.* B cells immortalized by a mini-Epstein-Barr virus encoding a foreign antigen efficiently reactivate specific cytotoxic T cells. *Blood* 2002; **100**: 1755–1764.
14 Kempkes B, Pich D, Zeidler R, Hammerschmidt W. Immortalization of human primary B lymphocytes *in vitro* with DNA. *Proc Natl Acad Sci USA* 1995; **92**: 5875–5879.
15 Kempkes B, Pich D, Zeidler R, Sugden B, Hammerschmidt W. Immortalization of human B lymphocytes by a plasmid containing 71 kilobase pairs of Epstein-Barr virus DNA. *J Virol* 1995; **69**: 231–238.
16 Delecluse HJ, Hilsendegen T, Pich D, Zeidler R, Hammerschmidt W. Propagation and recovery of intact, infectious Epstein-Barr virus from prokaryotic to human cells. *Proc Natl Acad Sci USA* 1998; **95**: 8245–8250.
17 Kilger E, Pecher G, Schwenk A, Hammerschmidt W. Expression of mucin (MUC-1) from a mini-Epstein-Barr virus in immortalized B-cells to generate tumor antigen specific cytotoxic T cells. *J Gene Med* 1999; **1**: 84–92.
18 Call KM, Glaser T, Ito CY, Buckler AJ, Pelletier J, Haber DA *et al.* Isolation and characterization of a zinc finger polypeptide gene at the human chromosome 11 Wilms' tumor locus. *Cell* 1990; **60**: 509–520.
19 Lee SB, Haber DA. Wilms tumor and the WT1 gene. *Exp Cell Res* 2001; **264**: 74–99.
20 Miwa H, Beran M, Saunders GF. Expression of the Wilms' tumor gene (WT1) in human leukemias. *Leukemia* 1992; **6**: 405–409.
21 Oka Y, Tsuboi A, Taguchi T, Osaki T, Kyo T, Nakajima H *et al.* Induction of WT1 (Wilms' tumor gene)-specific cytotoxic T lymphocytes by WT1 peptide vaccine and the resultant cancer regression. *Proc Natl Acad Sci USA* 2004; **101**: 13885–13890.
22 Kanda T, Yajima M, Ahsan N, Tanaka M, Takada K. Production of high-titer Epstein-Barr virus recombinants derived from Akata cells by using a bacterial artificial chromosome system. *J Virol* 2004; **78**: 7004–7015.
23 Kanda T, Shibata S, Saito S, Murata T, Isomura H, Yoshiyama H *et al.* Unexpected instability of family of repeats (FR), the critical cis-acting sequence required for EBV latent infection, in EBV-BAC systems. *PLoS One* 2011; **6**: e27758.
24 Graham FL, Smiley J, Russell WC, Nairn R. Characteristics of a human cell line transformed by DNA from human adenovirus type 5. *J Gen Virol* 1977; **36**: 59–74.
25 Haber DA, Sohn RL, Buckler AJ, Pelletier J, Call KM, Housman DE. Alternative splicing and genomic structure of the Wilms tumor gene WT1. *Proc Natl Acad Sci USA* 1991; **88**: 9618–9622.
26 Zhang Y, Muyrers JP, Testa G, Stewart AF. DNA cloning by homologous recombination in Escherichia coli. *Nat Biotechnol* 2000; **18**: 1314–1317.
27 Yasukawa M, Inatsuki A, Horiuchi T, Kobayashi Y. Functional heterogeneity among herpes simplex virus-specific human CD4+ T cells. *J Immunol* 1991; **146**: 1341–1347.
28 Okamoto S, Mineno J, Ikeda H, Fujiwara H, Yasukawa M, Shiku H *et al.* Improved expression and reactivity of transduced tumor-specific TCRs in human lymphocytes by specific silencing of endogenous TCR. *Cancer Res* 2009; **69**: 9003–9011.
29 Niwa H, Yamamura K, Miyazaki J. Efficient selection for high-expression transfectants with a novel eukaryotic vector. *Gene* 1991; **108**: 193–199.
30 Argast GM, Stephens KM, Emond MJ, Monnat Jr RJ. I-Ppol and I-CreI homing site sequence degeneracy determined by random mutagenesis and sequential *in vitro* enrichment. *J Mol Biol* 1998; **280**: 345–353.
31 Shaner NC, Campbell RE, Steinbach PA, Giepmans BN, Palmer AE, Tsien RY. Improved monomeric red, orange and yellow fluorescent proteins derived from Discosoma sp. red fluorescent protein. *Nat Biotechnol* 2004; **22**: 1567–1572.
32 Ohminami H, Yasukawa M, Fujita S. HLA class I-restricted lysis of leukemia cells by a CD8(+) cytotoxic T-lymphocyte clone specific for WT1 peptide. *Blood* 2000; **95**: 286–293.
33 Feederle R, Kost M, Baumann M, Janz A, Drouet E, Hammerschmidt W *et al.* The Epstein-Barr virus lytic program is controlled by the co-operative functions of two transactivators. *EMBO J* 2000; **19**: 3080–3089.
34 Wade-Martins R. Developing extrachromosomal gene expression vector technologies: an overview. *Methods Mol Biol* 2011; **738**: 1–17.
35 Kast WM, Levitsky H, Marincola FM. Synopsis of the 6th Walker's Cay colloquium on cancer vaccines and immunotherapy. *J Transl Med* 2004; **2**: 20.
36 Osada T, Woo CY, McKinney M, Yang XY, Lei G, Labreche HG *et al.* Induction of Wilms' tumor protein (WT1)-specific antitumor immunity using a truncated WT1-expressing adenovirus vaccine. *Clin Cancer Res* 2009; **15**: 2789–2796.

Cancer Science
The official journal of the Japanese Cancer Association

Antitumor activities of valproic acid on Epstein–Barr virus-associated T and natural killer lymphoma cells

Seiko Iwata,[1] Takashi Saito,[1] Yoshinori Ito,[2] Maki Kamakura,[1] Kensei Gotoh,[2] Jun-ichi Kawada,[3] Yukihiro Nishiyama[1] and Hiroshi Kimura[1,4]

Departments of [1]Virology and [2]Pediatrics, Nagoya University Graduate School of Medicine, Nagoya; [3]Department of Infection and Immunology, Aichi Children's Health and Medical Center, Aichi, Japan

(Received August 11, 2011/Revised October 17, 2011/Accepted October 17, 2011/Accepted manuscript online October 21, 2011/Article first published online November 22, 2011)

Epstein–Barr virus (EBV), which infects B cells, T cells, and natural killer (NK) cells, is associated with multiple lymphoid malignancies. Recently, histone deacetylase (HDAC) inhibitors have been reported to have anticancer effects against various tumor cells. In the present study, we evaluated the killing effect of valproic acid (VPA), which acts as an HDAC inhibitor, on EBV-positive and -negative T and NK lymphoma cells. Treatment of multiple T and NK cell lines (SNT13, SNT16, Jurkat, SNK6, KAI3 and KHYG1) with 0.1-5 mM of VPA inhibited HDAC, increased acetylated histone levels and reduced cell viability. No significant differences were seen between EBV-positive and -negative cell lines. Although VPA induced apoptosis in some T and NK cell lines (SNT16, Jurkat and KHYG1) and cell cycle arrest, it did not induce lytic infection in EBV-positive T or NK cell lines. Because the killing effect of VPA was modest (1 mM VPA reduced cell viability by between 22% and 56%), we tested the effects of the combination of 1 mM of VPA and 0.01 μM of the proteasome inhibitor bortezomib. The combined treated of cells with VPA and bortezomib had an additive killing effect. Finally, we administered VPA to peripheral blood mononuclear cells from three patients with EBV-associated T or NK lymphoproliferative diseases. In these studies, VPA had a greater killing effect against EBV-infected cells than uninfected cells, and the effect was increased when VPA was combined with bortezomib. These results indicate that VPA has antitumor effects on T and NK lymphoma cells and that VPA and bortezomib may have synergistic effects, irrespective of the presence of EBV. (*Cancer Sci* 2012; 103: 375–381)

The ubiquitous Epstein–Barr virus (EBV) infects most individuals by early adulthood and typically remains latent throughout life. Not only does EBV infect B cells, T cells, and natural killer (NK) cells, but it is also associated with multiple lymphoid malignancies, including Burkitt lymphoma, diffuse large B cell lymphoma, Hodgkin lymphoma, post-transplant lymphoproliferative disorders, nasal NK/T-cell lymphoma, hydroa vacciniforme-like lymphoma, aggressive NK cell leukemia, and chronic active EBV disease.[1–4] Epstein–Barr virus plays an important role in the pathogenesis of many of these malignancies via its ability to establish latent infection and induce the proliferation of infected cells.[5] Some of these EBV-associated lymphoid malignancies are refractory and resistant to conventional chemotherapies. Rituximab, a humanized monoclonal antibody against CD20, targets B cell-specific surface antigens present on EBV-transformed malignant cells. Currently, rituximab is used for the treatment and prophylaxis of B cell lymphoma and lymphoproliferative disorders.[6,7] However, the need remains for effective treatments for T and NK cell lymphoid malignancies and novel approaches to molecular targeting are desirable.

Sodium valproate (VPA) is a short chain fatty acid that is widely used to treat epilepsy. It is easily accessible and has a well-established safety profile. Recently, VPA was reported to be a potent histone deacetylase (HDAC) inhibitor and inducer of DNA demethylation.[8] It has been found that HDAC inhibitors have potent anticancer activities, with remarkable tumor specificity, and some have even demonstrated therapeutic potential.[9] The HDAC inhibitors can affect tumor cell growth and survival through multiple biological effects. For example, they induce tumor cell death with all of the biochemical and morphological characteristics of apoptosis. Several HDAC inhibitors have been used in the treatment of leukemias and lymphomas, such as cutaneous T cell lymphoma, myelodysplastic syndrome, and diffuse B cell lymphoma.[9] They have been used alone or in combination with DNA demethylating agents or other anticancer chemotherapies. Valproate has been reported to induce cell death in human leukemia cell lines[10] and endometrial tumor cells,[11] and to enhance the efficacy of chemotherapy in EBV-positive tumors.[12] Furthermore, VPA was shown to activate lytic viral gene expression in cells infected with EBV.[12,13]

Previously, we reported that the proteasome inhibitor bortezomib induced apoptosis in T and NK lymphoma cells.[14] Bortezomib produced a stronger killing effect in EBV-infected tumor cells compared with uninfected cells from patients with EBV-associated lymphoproliferative diseases, although the killing effect of bortezomib in cell lines was not affected by the presence of EBV. In the present study, we administered VPA to EBV-positive and -negative T cell lines and NK cell lines, and evaluated its antitumor effects by analyzing cell viability, the induction of apoptosis, cell cycle arrest, and expression of EBV-encoded genes. Finally, we evaluated the antitumor effect of the combination of VPA and bortezomib using both *in vitro* cell lines and *ex vivo* primary cultures of EBV-infected T and NK lymphoma cells.

Materials and Methods

Cell lines and reagents. Of the cell lines used in the present study, SNT13 and SNT16 are EBV-positive T cell lines,[15] SNK6[15] and KAI3[16] are EBV-positive NK cell lines, and Jurkat[17] and KHYG1[18] are EBV-negative T and NK cell lines, respectively. The SNT13, SNT16, SNK6, and KAI3 cells were derived from patients with chronic active EBV disease or nasal NK/T-cell lymphoma. The MT2/rEBV/9-7 cell line[19] was established through infection of MT2 cells with the hygromycin-resistant B95-8 strain.[20] The MT2/hyg cell line was transfected with a hygromycin resistance gene. Similarly, the NKL cell line[21] was derived from a patient with NK cell leukemia, and the TL1 cell line[22] was established from NKL cells infected with an Akata-transfected recombinant EBV strain carrying a neomycin resistance gene.

[4]To whom correspondence should be addressed.
E-mail: hkimura@med.nagoya-u.ac.jp

doi: 10.1111/j.1349-7006.2011.02127.x

Valproate (Sigma, St Louis, MO, USA) was dissolved in distilled water. Bortezomib, a gift from Millennium Pharmaceuticals (Cambridge, MA, USA), was dissolved in PBS.

Cell viability. Cell viability was quantified by Trypan blue exclusion. These experiments were performed in duplicate.

Immunoblotting. Cells were lysed directly in SDS sample buffer. Cell lysates were separated by SDS-PAGE, transferred to PVDF membranes, and immunoblotted with antibodies. Antibodies directed against acetyl-Histone 3, caspase-3, cleaved caspase-3, poly(ADP-ribose) polymerase (PARP; Cell Signaling Technology, Beverly, MA, USA), and β-actin (Sigma) were used.

Flow cytometry apoptosis assays. Apoptosis was measured by flow cytometry using an annexin V–phycoerythrin (PE)/7-aminoactinomycin D (7-AAD) apoptosis assay kit (BD Pharmingen Biosciences, San Diego, CA, USA) according to the manufacturer's instructions.

Cell cycle assay. Cells were treated with 1 mM of VPA for 48 h, fixed with 70% ethanol, and then washed with ice-cold PBS. Fixed cells were treated with 10 μg/mL DNase-free RNase and stained with 5 μg/mL propidium iodide (Sigma).

Real-time RT-PCR. Viral mRNA expression was quantified by RT-PCR, as described previously.[23,24] β2-Microglobulin (β2m) was used as an endogenous control and reference gene for relative quantification.[25] Each experiment was performed in triplicate. The Mann-Whitney *U*-test was used to compare expression levels and $P < 0.05$ were considered significant.

Patients. Mononuclear cells (MNC) were collected from three patients with EBV-associated diseases. Patients T-1 (a 7-year-old boy) and T-2 (a 6-year-old girl) had hydroa vacciniforme-like lymphoma, a newly classified EBV-associated T cell lymphoma.[2] In these patients, approximately 10% of the MNC were infected with EBV and the EBV-infected cells were primarily γδT cells.[26] The third patient, NK-1 (a 14-year-old boy), had chronic active EBV disease, NK cell type.[27–29] Chronic active EBV disease is now considered an EBV-associated T/NK lymphoproliferative disease.[30,31] In this patient, approximately 40% of the MNC were infected with EBV and the EBV-infected cells were NK cells. Mononuclear cells from three healthy donors were used as controls. Informed consent was obtained from all participants or their guardians. The present study was approved by the Institutional Review Board of Nagoya University Hospital.

Flow cytometric *in situ* hybridization (FISH). To quantify EBV-infected cells and to identify the cell type(s) infected by EBV, a FISH assay was performed.[26] Briefly, 5×10^5 MNC were stained with monoclonal antibodies for 1 h at 4°C. Cells were fixed, permeabilized, and hybridized with a fluorescein-labeled EBV-encoded small RNA (EBER)-specific peptide nucleic acid probe (Y5200; Dako, Glostrup, Denmark). Stained cells were analyzed using a FACSCalibur flow cytometer and CellQuest software (BD Biosciences, San Jose, CA, USA).

Magnetic cell sorting. Primarily infected cell fractions were separated by magnetic sorting using a TCRγ/δ$^+$ T Cell Isolation kit or CD56 MicroBeads (Miltenyi Biotec, Bergisch Gladbach, Germany). The purity and recovery rates were 98.3% and 80.0%, respectively, with the TCRγ/δ$^+$ T Cell Isolation kit, and 96.4% and 80.9%, respectively, with the CD56 MicroBeads.

Results

Effects of VPA on HDAC in T and NK cell lines. Acetylated histone 3 levels were determined in T cell lines (SNT16 and Jurkat) and NK cell lines (KAI3 and KHYG1) after 24 h exposure to 0.1-5 mM of VPA. Valproate increased acetylated histone 3 levels in a dose-dependent manner (Fig. 1a), indicating that VPA inhibits HDAC in these cell lines.

Effects of VPA on the viability of T and NK cell lines. To evaluate the effects of VPA on cells viability, EBV-positive T cell lines (SNT13 and SNT16), an EBV-negative T cell line (Jurkat), EBV-positive NK cell lines (KAI3 and SNK6), and an EBV-negative NK cell line (KHYG1) were exposed to 0.1-5 mM of VPA for 24 h. The cell viability of all six cell lines tested was reduced by VPA in a dose-dependent manner (Fig. 1b,d). In another series of experiments, the same six cell lines were exposed to 1 mM VPA for 4 days, with viability evaluated every 24 h. In these experiments, VPA reduced the viability of all six cell lines by between 22% and 52% after 96 h (Fig. 1c,e). There were no obvious differences between the effects of VPA on EBV-positive and -negative cell lines. Furthermore, to directly compare the effects of VPA on EBV-positive and -negative cell lines, we exposed MT2/hyg and MT2/rEBV/9-7 (Fig. 1f,g) and NKL and TL1 (Fig. 1h,i) cells to VPA and found that 0.1-5 mM of VPA had almost identical effects on the EBV-positive and -negative cell lines.

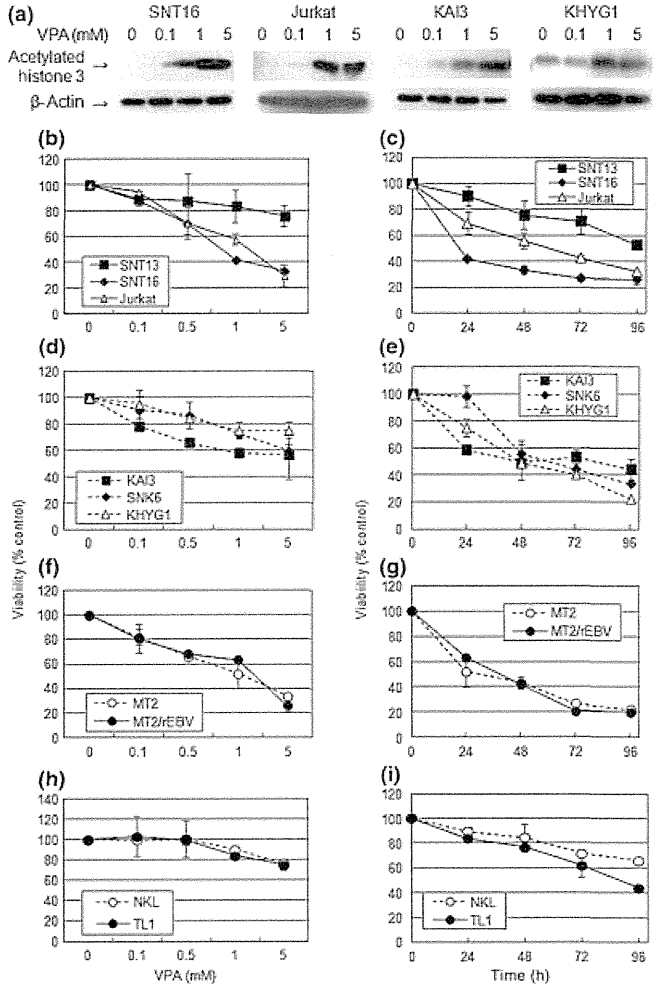

Fig. 1. Valproate (VPA) inhibits histone deacetylase (HDAC) and reduces viability of T and natural killer (NK) cell lines. (a) Acetylated histone 3 was detected by immunoblotting in T and NK cell lines treated with various concentrations of VPA for 24 h. β-Actin was used as a loading control. Viability of (b,c) Epstein–Barr virus (EBV)-positive T cell lines (SNT13 and SNT16) and an EBV-negative T cell line (Jurkat), (d,e) EBV-positive NK cell lines (KAI3 and SNK6) and an EBV-negative NK cell line (KHYG1), (f,g) an EBV-positive T cell line (MT2/rEBV) and its parental cell line (MT2/hyg), and (h,i) an EBV-positive NK cell line (TL1) and its parental line (NKL) that were either treated with VPA at the concentrations indicated for 24 h (b,d,f,h) or with 1 mM VPA for 96 h (c,e,g,i). Viability is shown as the ratio of viable cells in the different treatment groups to distilled water-treated cells, as assessed by Trypan blue exclusion. Data are the mean ± SEM.

doi: 10.1111/j.1349-7006.2011.02127.x

Effects of VPA on the apoptosis of T and NK cell lines. To determine whether VPA induces apoptosis in these cell lines, the cleavage of caspase-3 and PARP was analyzed by immunoblotting. One mM of VPA increased levels of cleaved caspase-3 and PARP in Jurkat and KHYG1, which are EBV-negative T and NK cell lines, respectively (Fig. 2a), suggesting that VPA induces apoptosis in these two cell lines. Analysis of the induction of apoptosis by flow cytometry showed that VPA only increased the number of apoptotic cells in the SNT16 cell line (Fig. 2b). In the other cell lines tested, increases in the number of apoptotic cells were not confirmed, although the number of dead cells increased. A representative result for KHYG1 cells is shown in Figure 2(c).

Effects of VPA on the cell cycle in T and NK cell lines. To investigate the effects of VPA on the cell cycle, cells were treated with 1 mM VPA for 48 h, stained with propidium iodide, and then analyzed by flow cytometry. The population of cells in the G_1 phase was increased following exposure

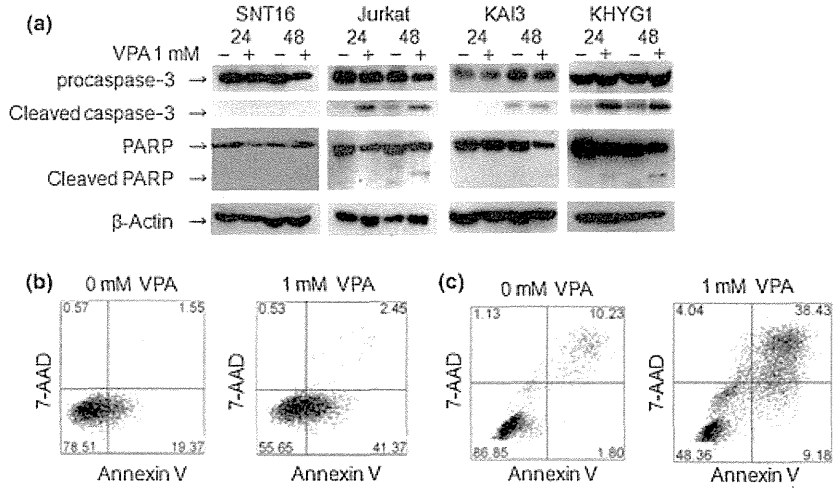

Fig. 2. Effects of valproate (VPA) on apoptosis. (a) T and natural killer (NK) cell lines were treated with 1 mM VPA for 24 or 48 h. β-Actin was used as a loading control. Valproate induced the cleavage of caspase-3 and poly (ADP-ribose) polymerase (PARP) in Jurkat and KHYG1 cells. (b,c) T and NK cell lines were treated with 1 mM VPA for 48 h. Viable cells were defined as those negative for annexin V–phycoerythrin (PE) and 7-amino-actinomycin D (7-AAD). (b) The number of early apoptotic SNT16 cells, defined as those positive for annexin V-PE and negative for 7-AAD, was increased, as was (c) the numbers of dead KHYG1 cells, defined as those positive for both annexin V-PE and 7-AAD.

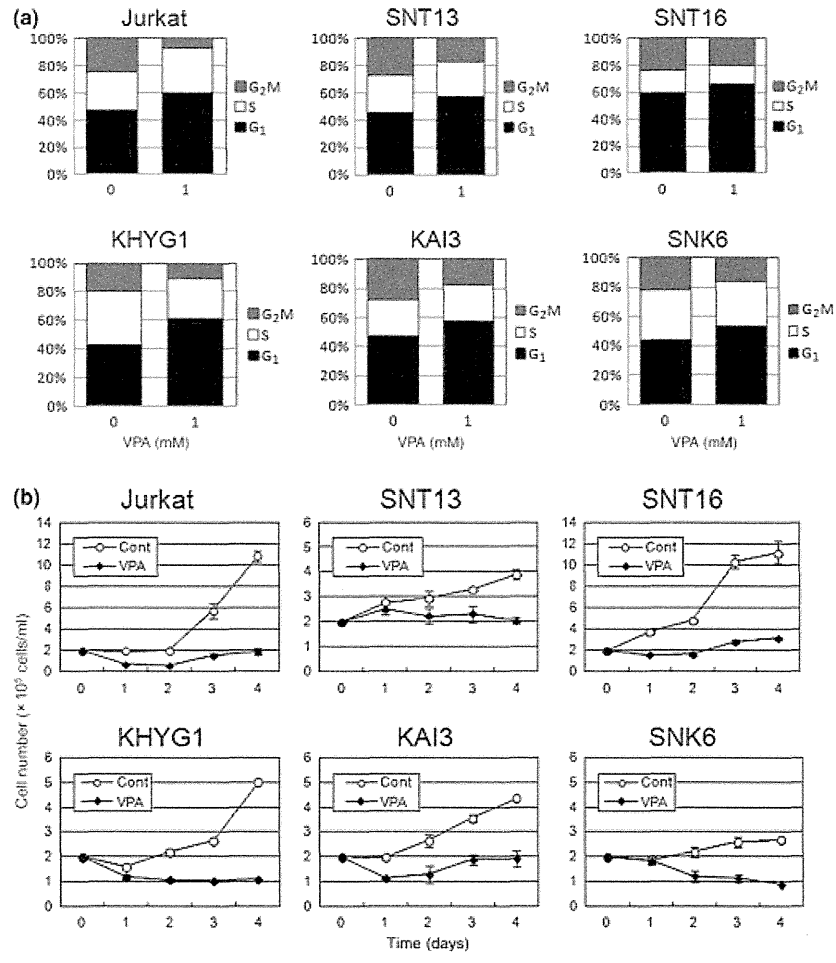

Fig. 3. Effects of valproate (VPA) on the cell cycle. (a) T cell lines (SNT13, SNT16, and Jurkat), and natural killer (NK) cell lines (KAI3, SNK6, and KHYG1) were treated with 1 mM VPA or distilled water for 48 h, fixed, and stained with propidium iodide. Cell cycle profiles were assessed by flow cytometry. (b) Cells were treated with 1 mM VPA or distilled water (control) and viable cells were counted using the Trypan blue exclusion test. Experiments were performed in duplicate. Data are the mean ± SEM.

to VPA and VPA arrested the cell cycle in all T and NK cell lines tested (Fig. 3a). To confirm that VPA arrested the cell cycle, proliferation was compared in the presence and absence of VPA. Proliferation was inhibited in all VPA-treated cells compared with control cells (Fig. 3b).

Effects of VPA on lytic infection of EBV-positive T and NK cell lines. The expression of the following eight viral genes were analyzed using real-time RT-PCR: lytic genes encoding BZLF1 and gp350/220; and latent genes encoding EBV nuclear antigen (EBNA) 1, EBNA2, latent membrane protein (LMP) 1, LMP2, EBER1, and *Bam*HI-A rightward transcripts (BARTs). BZLF1, but not gp350/220, was detected in the T cell lines. Conversely, neither BZLF1 nor gp350/220 were detected in the NK cell lines (Fig. 4). The expression of the two lytic genes and six latent genes did not differ significantly between VPA-treated cells and controls. Representative results for two latent genes (those encoding LMP1 and EBER1) are shown in Figure 4.

Effects of the combination of VPA and bortezomib on cell death. Because the antitumor effect of VPA alone was modest (1 mM VPA treatment for 96 h reduced cell viability by between 22% and 56%) (Fig. 1b–e), we evaluated the effects of the combination of VPA (1 mM) and the proteasome inhibitor bortezomib (0.01 μM) in several cell lines. In Jurkat and KAI3 cells, the combination of VPA plus bortezomib enhanced cell death (Fig. 5); however, in SNT16 and KHYG1 cells, the effects of this combination were difficult to assess because 0.01 μM bortezomib alone killed almost all the cells (Fig. 5).

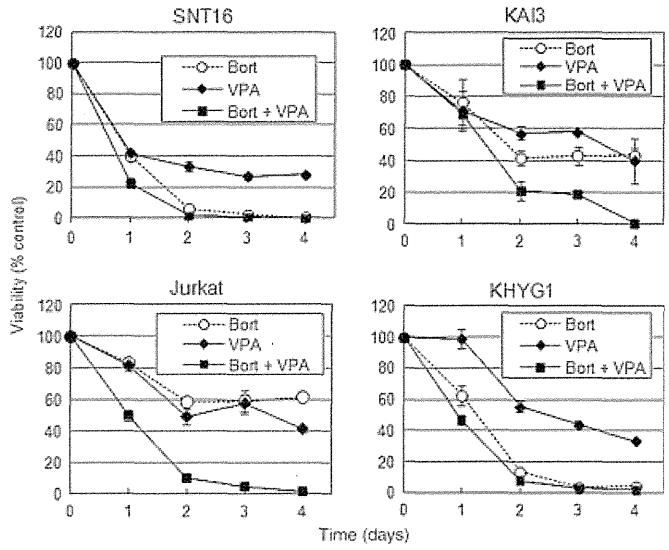

Fig. 5. Combined effects of valproate (VPA) and bortezomib. T cell lines (SNT16 and Jurkat) and natural killer (NK) cell lines (KAI3 and KHYG1) were treated with 1 mM VPA and/or 0.01 μM bortezomib for 96 h and cell viability was assessed. VPA and bortezomib had additive effects in reducing the viability of T and NK cell lines. Data are the mean ± SEM.

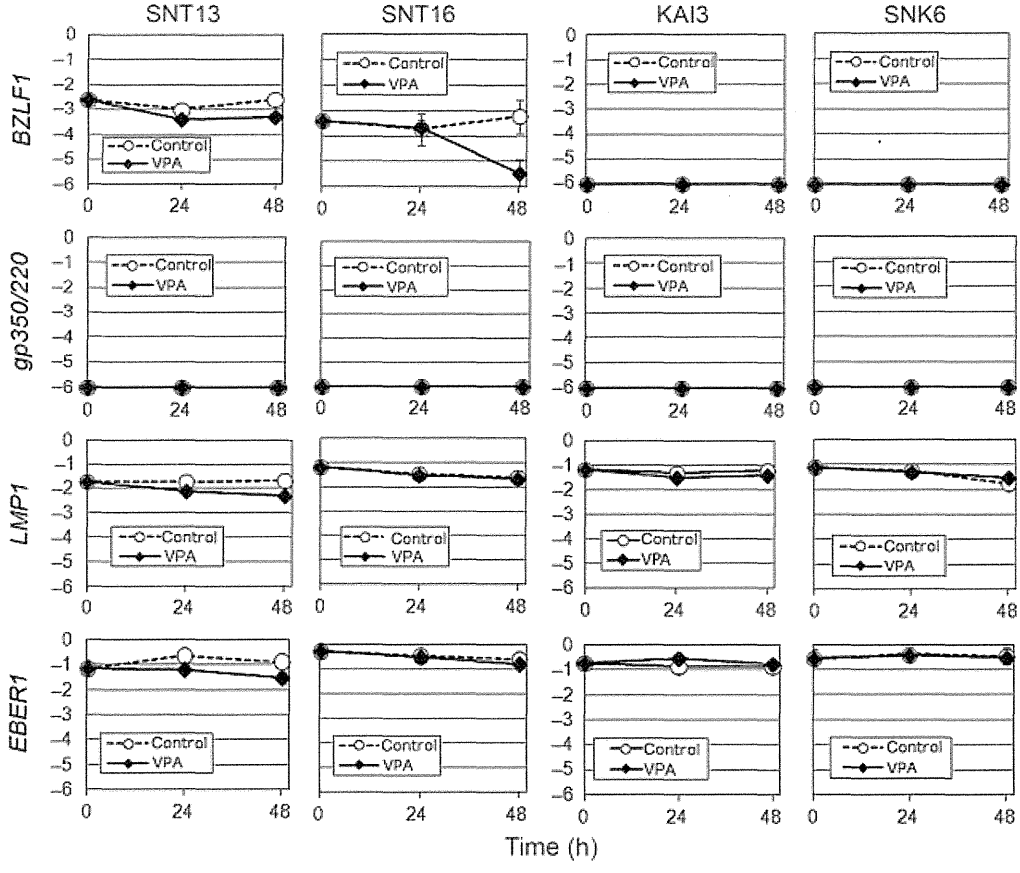

Fig. 4. Effects of valproate (VPA) treatment on the expression of Epstein–Barr virus (EBV)-encoded genes. The EBV-positive T cell lines (SNT13 and SNT16) and EBV-positive natural killer (NK) cell lines (KAI3 and SNK6) were treated with 1 mM VPA and harvested at 0, 24, and 48 h to evaluate gene expression using real-time RT-PCR. *BZLF1* is an immediate early gene and *gp350/220* is a late gene. *LMP1* and *EBER1* are latent genes. β2-Microglobulin was used as an internal control and reference gene for relative quantification and assigned an arbitrary value of 1 (10^0). Data are the mean ± SEM.

doi: 10.1111/j.1349-7006.2011.02127.x

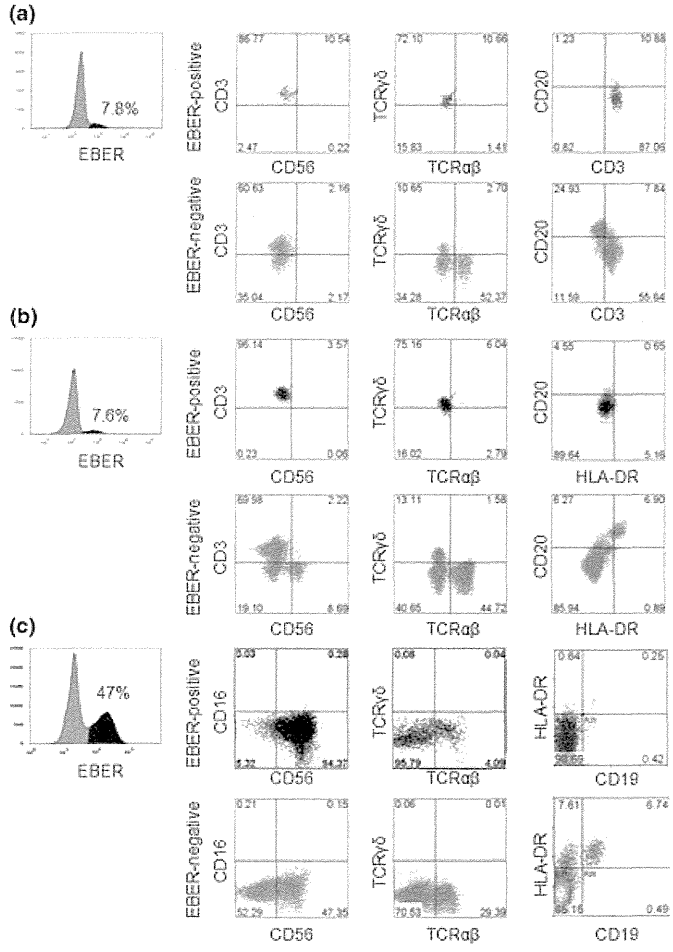

Fig. 6. Identification of Epstein–Barr virus (EBV)-infected cell fractions in patients with EBV-associated T/natural killer (NK) lymphoma. (a, b) Patients T-1 (a) and T-2 (b), who had hydroa vacciniforme-like lymphoma. (c) Patient NK-1, who had chronic active EBV disease, NK cell-type. Mononuclear cells were analyzed in a FISH assay. The EBV-encoded small RNA (EBER)-positive (black) and -negative (gray) lymphocytes were gated and plotted in quadrants.

Effects of VPA on the viability of EBV-infected cells from patients with EBV-associated lymphoma. The *ex vivo* effect of VPA on lymphoma cells from patients with EBV-associated T/NK lymphoma or lymphoproliferative diseases was evaluated. To identify the fractions that contained EBV-infected cells, MNC were stained with surface marker antibodies and then subjected to *in situ* hybridization with EBER in a FISH assay. In patients T-1 and T-2, who had hydroa vacciniforme-like lymphoma, the FISH assay showed that 7.8% and 7.6% of MNC were EBER positive, respectively. Most of the EBER-positive MNC in these patients were CD3+ and TCRγδ+ T cells (Fig. 6a,b). Conversely, in patient NK-1, who had chronic active EBV disease, 47% of MNC were EBER positive. Most of the EBER-positive MNC in this patient were CD56+ NK cells (Fig. 6c). Magnetic sorting was then used to separated γδT cells from other MNC in patients T-1 and T-2, and NK cells from the other MNC in patient NK-1. Bortezomib (0.5 μM) and/or VPA (1 mM) was administered to each fraction and viable cells were counted over a period of 3–4 days. Individually, bortezomib and VPA had greater killing effects on the fractions containing EBV-infected cells compared with the other MNC, whereas the combination of bortezomib plus VPA produced the strongest killing effect (Fig. 7a–c). In the γδT and NK cell fractions, the absolute number of control viable cells was stable or increased slightly, but was reduced by treatment (data not shown). The viability of cells obtained from blood samples from three healthy donors after combined treatment with bortezomib plus VPA for 4 days ranged between 75% and 100%, indicating that bortezomib and VPA do not affect non-tumor cells (Fig. 7d).

Discussion

Several studies have reported that HDAC inhibitors have anticancer activities and some have even been tested in clinical trials.[32–34] Valproate is used to treat epilepsy, is easily accessible, and has a well-established safety profile. Therefore, evaluation of an anticancer effect of VPA may be very useful in the treatment of malignant diseases. In the present study, VPA reduced the viability of T and NK lymphoma/leukemia cell lines independently of the presence of EBV. However, the killing effect of VPA was smaller than that of bortezomib, despite the fact that the concentration of VPA tested (1 mM) was higher than that used in the treatment of epilepsy (0.3–0.6 mM).

The HDAC inhibitors affect tumor cell growth and survival via multiple biological effects. For example, they induce tumor cell death with all the biochemical and morphological characteristics of apoptosis. The HDAC inhibitors induce cell cycle arrest at the G_1/S boundary via upregulation of *CDKN1A*, which encodes $p21^{WAF1/CIP1}$, and/or downregulation of cyclins. They can suppress angiogenesis by reducing the expression of proangiogenic factors and also have immunomodulatory effects, enhancing tumor cell antigenicity and altering the expression of key cytokines, including tumor necrosis factor-α, interleukin-1, and interferon-γ.[9] In the present study, we analyzed the mechanism by which VPA reduces the viability of T and NK cell lines. In some cell lines, VPA induced apoptosis, whereas in most there was evidence of cell cycle arrest. Thus, VPA probably activates other pathways to kill tumor cells than apoptosis and cell cycle arrest.

The proteasome inhibitor bortezomib has strong killing effects on T and NK lymphoma/leukemia cell lines (independent of the presence of EBV) and EBV-infected tumor cells from patients with EBV-associated T/NK lymphoproliferative diseases.[14] Bortezomib is used in the treatment of myeloma and has also been assessed for efficacy against a variety of other malignancies. Recently, bortezomib and an HDAC inhibitor were reported to have synergistic effects in human and mouse models.[35,36] Therefore, in the present study we evaluated the effects of the combination of bortezomib and VPA. Bortezomib and VPA were found to have additive killing effects on T and NK cell lines and EBV-infected MNC from patients. In the two cell lines tested, the effect of bortezomib was too strong to evaluate the killing effect of the combination treatment, despite the low bortezomib concentration used. Conversely, in Jurkat and KAI3, in which a low concentration of bortezomib killed approximately half the cells, the combination treatment killed nearly all cells within 4 days. Furthermore, the combination treatment had a stronger killing effect in EBV-infected MNC from patients than in uninfected cells. These results suggest the potential usefulness of the combination of VPA and bortezomib in the treatment of EBV-associated T/NK lymphoproliferative diseases.

Valproate has been reported to induce lytic infection by EBV,[12,13] human cytomegalovirus,[37] and Kaposi sarcoma-associated herpes virus.[38] Induction of the lytic cycle is an advantage for the treatment of EBV-associated malignant diseases because of the lysis of EBV-infected tumor cells, the possible availability of antiviral therapy, and the recognition of expressed viral lytic proteins by the host immune system. Furthermore, the combination of VPA and an antiviral drug may

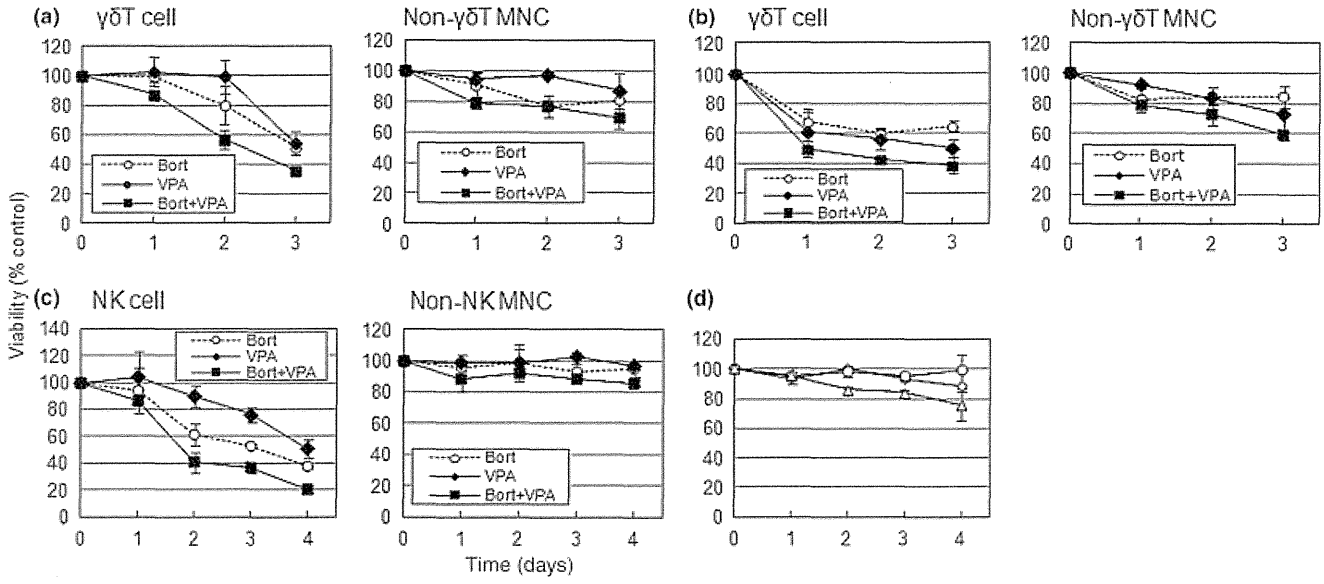

Fig. 7. Effects of the combination of valproate (VPA) and bortezomib on Epstein–Barr virus (EBV)-infected lymphoma cells. Cell populations were separated by magnetic sorting. Each fraction was exposed to VPA (1 mM) and/or bortezomib (0.5 μM) and viable cells were counted over 3 or 4 days. (a,b) Viability of γδT cells and other mononuclear cells (MNC) from patients T-1 (a) and T-2 (b) with hydroa vacciniforme-like lymphoma. (c) Viability of NK cells and other MNC from patient NK-1 with chronic active EBV disease, NK cell-type. (d) Viability of MNC from three healthy donors treated with 1 mM VPA and 0.5 μM bortezomib for 4 days. Data are the mean ± SEM.

increase cell killing because some antiviral drugs inhibit virus DNA polymerase and are more effective in the lytic state than in the latent state.[39] To our knowledge, this is the first report of the effects of VPA on T and NK cell lines. In previous studies showing that VPA induces the EBV lytic cycle, a gastric carcinoma cell line and B cell lines were used.[12,13] In the present study, VPA did not induce the EBV lytic cycle in any of the T or NK cell lines tested. In the two EBV-positive T cell lines tested, expression of only the immediate early gene *BZLF1* was detected (expression of the late gene *gp350/220* was not detected). In the NK cell lines, the expression of neither gene was detected. These results are consistent with our previous report.[23] In addition, bortezomib only induced the EBV lytic cycle in EBV-positive T cell lines.[23] Therefore, it seems that lytic infection can be induced in EBV-positive T cell lines. Nevertheless, VPA treatment did not induce lytic infection in EBV-positive T cell lines in the present study.

In summary, the results of the present study suggest that VPA has potential antitumor activity, regardless of whether EBV is present, although its efficacy may not be sufficient. The combination of VPA plus bortezomib may be a useful treatment because of the potential synergistic effects. Our results indicate that VPA has killing effects on T and NK lymphoma cells. Other HDAC inhibitors, such as suberoylanilide hydroxamic acid and depsipeptide, have potent activity against T cell lymphoma[40] and may produce beneficial effects in EBV-associated malignancies by inducing the lytic cycle or suppressing the expression of EBV-related genes.[13]

Acknowledgments

The authors thank Shigeyoshi Fujiwara (National Research Institute for Child Health and Development, Tokyo, Japan) for the MT2/hyg and MT2/rEBV/9-7 cell lines and Koichi Sugimoto and Yasushi Isobe (Juntendo University, Tokyo, Japan) for the NKL and TL1 cell lines. The KAI3 and KHYG1 cells were obtained from the Japanese Collection of Research Bioresources (Osaka, Japan). The authors thank Millennium Pharmaceuticals (Cambridge, MA, USA) for providing the bortezomib. This study was supported, in part, by a grant from the Ministry of Education, Culture, Sports, Science and Technology, Japan (19591247) and by a grant for Research on Measures for Emerging and Reemerging Infections (Intractable Infectious Diseases in Organ Transplant Recipients, H21-Shinko-Ippan-094) from the Ministry of Health, Labor, and Welfare of Japan.

Disclosure Statement

The authors have no conflict of interest.

References

1 Cohen JI. Epstein–Barr virus infection. *N Engl J Med* 2000; **343**: 481–92.
2 Quintanilla-Martinez L, Kimura H, Jaffe ES. EBV+ T-cell lymphoma of childhood. In: Jaffe ES, Harris NL, Stein H, eds. *WHO Classification of Tumours of Haematopoietic and Lymphoid Tissues*, 4th edn. Lyon: IARC Press, 2008; 278–80.
3 Rickinson AB, Kieff E. Epstein–Barr virus. In: Knipe DM, Howley PM, eds. *Fields Virology*. Philadelphia: Lippincott Williams & Wilkins, 2007; 2655–700.
4 Williams H, Crawford DH. Epstein–Barr virus: the impact of scientific advances on clinical practice. *Blood* 2006; **107**: 862–9.
5 Kieff ED, Rickinson AV. Epstein–Barr virus and its replication. In: Knipe DM, Howley PM, eds. *Fields Virology*. Philadelphia: Lippincott Williams & Wilkins, 2007; 2603–54.
6 Cartron G, Watier H, Golay J, Solal-Celigny P. From the bench to the bedside: ways to improve rituximab efficacy. *Blood* 2004; **104**: 2635–42.
7 Heslop HE. How I treat EBV lymphoproliferation. *Blood* 2009; **114**: 4002–8.
8 Detich N, Bovenzi V, Szyf M. Valproate induces replication-independent active DNA demethylation. *J Biol Chem* 2003; **278**: 27586–92.
9 Bolden JE, Peart MJ, Johnstone RW. Anticancer activities of histone deacetylase inhibitors. *Nat Rev Drug Discov* 2006; **5**: 769–84.
10 Kawagoe R, Kawagoe H, Sano K. Valproic acid induces apoptosis in human leukemia cells by stimulating both caspase-dependent and -independent apoptotic signaling pathways. *Leuk Res* 2002; **26**: 495–502.
11 Takai N, Desmond JC, Kumagai T *et al.* Histone deacetylase inhibitors have a profound antigrowth activity in endometrial cancer cells. *Clin Cancer Res* 2004; **10**: 1141–9.

doi: 10.1111/j.1349-7006.2011.02127.x

12 Feng WH, Kenney SC. Valproic acid enhances the efficacy of chemotherapy in EBV-positive tumors by increasing lytic viral gene expression. *Cancer Res* 2006; **66**: 8762–9.
13 Hui KF, Chiang AK. Suberoylanilide hydroxamic acid induces viral lytic cycle in Epstein–Barr virus-positive epithelial malignancies and mediates enhanced cell death. *Int J Cancer* 2010; **126**: 2479–89.
14 Iwata S, Yano S, Ito Y *et al.* Bortezomib induces apoptosis in T lymphoma cells and natural killer lymphoma cells independent of Epstein–Barr virus infection. *Int J Cancer* 2011; **129**: 2263–73.
15 Zhang Y, Nagata H, Ikeuchi T *et al.* Common cytological and cytogenetic features of Epstein–Barr virus (EBV)-positive natural killer (NK) cells and cell lines derived from patients with nasal T/NK-cell lymphomas, chronic active EBV infection and hydroa vacciniforme-like eruptions. *Br J Haematol* 2003; **121**: 805–14.
16 Tsuge I, Morishima T, Morita M, Kimura H, Kuzushima K, Matsuoka H. Characterization of Epstein–Barr virus (EBV)-infected natural killer (NK) cell proliferation in patients with severe mosquito allergy; establishment of an IL-2-dependent NK-like cell line. *Clin Exp Immunol* 1999; **115**: 385–92.
17 Kaplan J, Tilton J, Peterson WD Jr. Identification of T cell lymphoma tumor antigens on human T cell lines. *Am J Hematol* 1976; **1**: 219–23.
18 Yagita M, Huang CL, Umehara H *et al.* A novel natural killer cell line (KHYG-1) from a patient with aggressive natural killer cell leukemia carrying a p53 point mutation. *Leukemia* 2000; **14**: 922–30.
19 Miyoshi I, Kubonishi I, Yoshimoto S *et al.* Type C virus particles in a cord T-cell line derived by co-cultivating normal human cord leukocytes and human leukaemic T cells. *Nature* 1981; **294**: 770–1.
20 Fujiwara S, Ono Y. Isolation of Epstein–Barr virus-infected clones of the human T-cell line MT-2: use of recombinant viruses with a positive selection marker. *J Virol* 1995; **69**: 3900–3.
21 Robertson MJ, Cochran KJ, Cameron C, Le JM, Tantravahi R, Ritz J. Characterization of a cell line, NKL, derived from an aggressive human natural killer cell leukemia. *Exp Hematol* 1996; **24**: 406–15.
22 Isobe Y, Sugimoto K, Matsuura I, Takada K, Oshimi K. Epstein–Barr virus renders the infected natural killer cell line, NKL resistant to doxorubicin-induced apoptosis. *Br J Cancer* 2008; **99**: 1816–22.
23 Iwata S, Wada K, Tobita S *et al.* Quantitative analysis of Epstein–Barr virus (EBV)-related gene expression in patients with chronic active EBV infection. *J Gen Virol* 2010; **91**: 42–50.
24 Kubota N, Wada K, Ito Y *et al.* One-step multiplex real-time PCR assay to analyse the latency patterns of Epstein–Barr virus infection. *J Virol Methods* 2008; **147**: 26–36.
25 Patel K, Whelan PJ, Prescott S *et al.* The use of real-time reverse transcription-PCR for prostate-specific antigen mRNA to discriminate between blood samples from healthy volunteers and from patients with metastatic prostate cancer. *Clin Cancer Res* 2004; **10**: 7511–9.
26 Kimura H, Miyake K, Yamauchi Y *et al.* Identification of Epstein–Barr virus (EBV)-infected lymphocyte subtypes by flow cytometric in situ hybridization in EBV-associated lymphoproliferative diseases. *J Infect Dis* 2009; **200**: 1078–87.
27 Kimura H, Hoshino Y, Hara S *et al.* Differences between T cell-type and natural killer cell-type chronic active Epstein–Barr virus infection. *J Infect Dis* 2005; **191**: 531–9.
28 Kimura H, Hoshino Y, Kanegane H *et al.* Clinical and virologic characteristics of chronic active Epstein–Barr virus infection. *Blood* 2001; **98**: 280–6.
29 Kimura H, Morishima T, Kanegane H *et al.* Prognostic factors for chronic active Epstein–Barr virus infection. *J Infect Dis* 2003; **187**: 527–33.
30 Cohen JI, Kimura H, Nakamura S, Ko YH, Jaffe ES. Epstein–Barr virus-associated lymphoproliferative disease in non-immunocompromised hosts: a status report and summary of an international meeting, 8–9 September 2008. *Ann Oncol* 2009; **20**: 1472–82.
31 Kimura H. Pathogenesis of chronic active Epstein–Barr virus infection: is this an infectious disease, lymphoproliferative disorder, or immunodeficiency? *Rev Med Virol* 2006; **16**: 251–61.
32 Fakih MG, Fetterly G, Egorin MJ *et al.* A Phase I, pharmacokinetic, and pharmacodynamic study of two schedules of vorinostat in combination with 5-fluorouracil and leucovorin in patients with refractory solid tumors. *Clin Cancer Res* 2010; **16**: 3786–94.
33 Kirschbaum M, Frankel P, Popplewell L *et al.* Phase II Study of vorinostat for treatment of relapsed or refractory indolent non-Hodgkin's lymphoma and mantle cell lymphoma. *J Clin Oncol* 2011; **29**: 1198–203.
34 Niesvizky R, Ely S, Mark T *et al.* Phase 2 trial of the histone deacetylase inhibitor romidepsin for the treatment of refractory multiple myeloma. *Cancer* 2011; **117**: 336–42.
35 Jagannath S, Dimopoulos MA, Lonial S. Combined proteasome and histone deacetylase inhibition: a promising synergy for patients with relapsed/refractory multiple myeloma. *Leuk Res* 2010; **34**: 1111–8.
36 Kawada J, Zou P, Mazitschek R, Bradner JE, Cohen JI. Tubacin kills Epstein–Barr virus (EBV)–Burkitt lymphoma cells by inducing reactive oxygen species and EBV lymphoblastoid cells by inducing apoptosis. *J Biol Chem* 2009; **284**: 17102–9.
37 Kuntz-Simon G, Obert G. Sodium valproate, an anticonvulsant drug, stimulates human cytomegalovirus replication. *J Gen Virol* 1995; **76**: 1409–15.
38 Klass CM, Krug LT, Pozharskaya VP, Offermann MK. The targeting of primary effusion lymphoma cells for apoptosis by inducing lytic replication of human herpesvirus 8 while blocking virus production. *Blood* 2005; **105**: 4028–34.
39 Bazarbachi A, Suarez F, Fields P, Hermine O. How I treat adult T-cell leukemia/lymphoma. *Blood* 2011; **118**: 1736–45.
40 Zain JM, O'Connor O. Targeted treatment and new agents in peripheral T-cell lymphoma. *Int J Hematol* 2010; **92**: 33–44.